NASA/TM–2006–214501

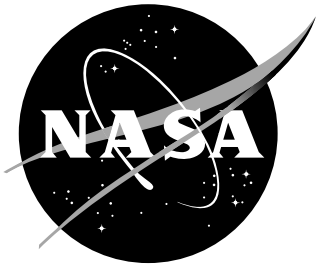

Control Laws for a Wind Tunnel Free-Flight Study of a Blended-Wing-Body Aircraft

E. Bruce Jackson and C. W. Buttrill
Langley Research Center, Hampton, Virginia

August 2006

The NASA STI Program Office ... in Profile

Since its founding, NASA has been dedicated to the advancement of aeronautics and space science. The NASA Scientific and Technical Information (STI) Program Office plays a key part in helping NASA maintain this important role.

The NASA STI Program Office is operated by Langley Research Center, the lead center for NASA's scientific and technical information. The NASA STI Program Office provides access to the NASA STI Database, the largest collection of aeronautical and space science STI in the world. The Program Office is also NASA's institutional mechanism for disseminating the results of its research and development activities. These results are published by NASA in the NASA STI Report Series, which includes the following report types:

- TECHNICAL PUBLICATION. Reports of completed research or a major significant phase of research that present the results of NASA programs and include extensive data or theoretical analysis. Includes compilations of significant scientific and technical data and information deemed to be of continuing reference value. NASA counterpart of peer-reviewed formal professional papers, but having less stringent limitations on manuscript length and extent of graphic presentations.
- TECHNICAL MEMORANDUM. Scientific and technical findings that are preliminary or of specialized interest, e.g., quick release reports, working papers, and bibliographies that contain minimal annotation. Does not contain extensive analysis.
- CONTRACTOR REPORT. Scientific and technical findings by NASA-sponsored contractors and grantees.
- CONFERENCE PUBLICATION. Collected papers from scientific and technical conferences, symposia, seminars, or other meetings sponsored or co-sponsored by NASA.
- SPECIAL PUBLICATION. Scientific, technical, or historical information from NASA programs, projects, and missions, often concerned with subjects having substantial public interest.
- TECHNICAL TRANSLATION. English-language translations of foreign scientific and technical material pertinent to NASA's mission.

Specialized services that complement the STI Program Office's diverse offerings include creating custom thesauri, building customized databases, organizing and publishing research results ... even providing videos.

For more information about the NASA STI Program Office, see the following:

- Access the NASA STI Program Home Page at ***http://www.sti.nasa.gov***
- E-mail your question via the Internet to help@sti.nasa.gov
- Fax your question to the NASA STI Help Desk at (301) 621–0134
- Phone the NASA STI Help Desk at (301) 621–0390
- Write to:
  NASA STI Help Desk
  NASA Center for AeroSpace Information
  7121 Standard Drive
  Hanover, MD 21076–1320

NASA/TM–2006–214501

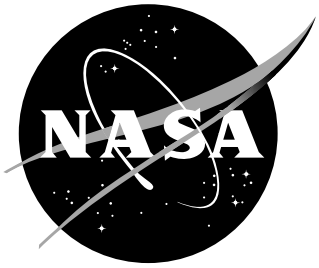

Control Laws for a Wind Tunnel Free-Flight Study of a Blended-Wing-Body Aircraft

E. Bruce Jackson and C. W. Buttrill
Langley Research Center, Hampton, Virginia

National Aeronautics and
Space Administration

Langley Research Center
Hampton, Virginia 23681-2199

August 2006

Acknowledgments

The authors extend their thanks to Dana McMinn, John Davidson, and Joe Pahle for previous work in this area, specifically the X-48A Ascender Low-Speed Vehicle RPV project; to Dan Vicroy for having faith in our abilities; to Dan Murri, Mark Croom, Jay Brandon for their many suggestions and for doing an excellent job in piloting the model without damage; to Charlie Debro and Gene Adams for putting all the hardware together and to Sue Grafton for making it all happen.

Available from:

NASA Center for AeroSpace Information (CASI)
7121 Standard Drive
Hanover, MD 21076–1320
(301) 621–0390

National Technical Information Service (NTIS)
5285 Port Royal Road
Springfield, VA 22161–2171
(703) 605–6000

Abstract

This paper documents the control laws used in the free-flight tests of a 5% scaled blended-wing-body aircraft in the NASA Langley 30x60 Full-Scale Tunnel, conducted in the summer of 2005.

Symbols

M	aerodynamic pitching moment
p	body-axis roll rate
Q	dynamic pressure
q	body-axis pitch rate
r	body-axis yaw rate
$\vec{r}$	position offset vector
s	Laplace operator
T	incremental time step size of digital control system
U	generic measurement
$\dot{U}$	time-rate-of-change of generic measurement
$\hat{U}$	estimated value of generic measurement
u	x-body axis velocity relative to freestream, positive forward
v	y-body axis velocity relative to freestream, positive right
V	velocity relative to freestream
w	z-body axis velocity relative to freestream, positive down
z	discrete operator
α	angle-of-attack
$\hat{\alpha}$	estimated angle-of-attack
β	angle-of-sideslip
$\hat{\beta}$	estimated angle-of-sideslip
τ	time constant of filter
$\vec{\omega}$	body-axis rotation vector

Subscripts

α	partial derivative with respect to angle-of-attack
cg	estimated at center of mass
$dist$	command distribution vector
$filt$	filtered measurement
$induced$	error caused by rotation of vehicle
n	current frame time measurement or calculation
$n-1$	previous frame time measurement or calculation
$sensed$	measurement obtained from a sensor

Acronyms

ARI	aileron-to-rudder interconnect
BWB	blended-wing-body configuration
C.G.	center of gravity
DA	aileron deflection
DE	elevator deflection

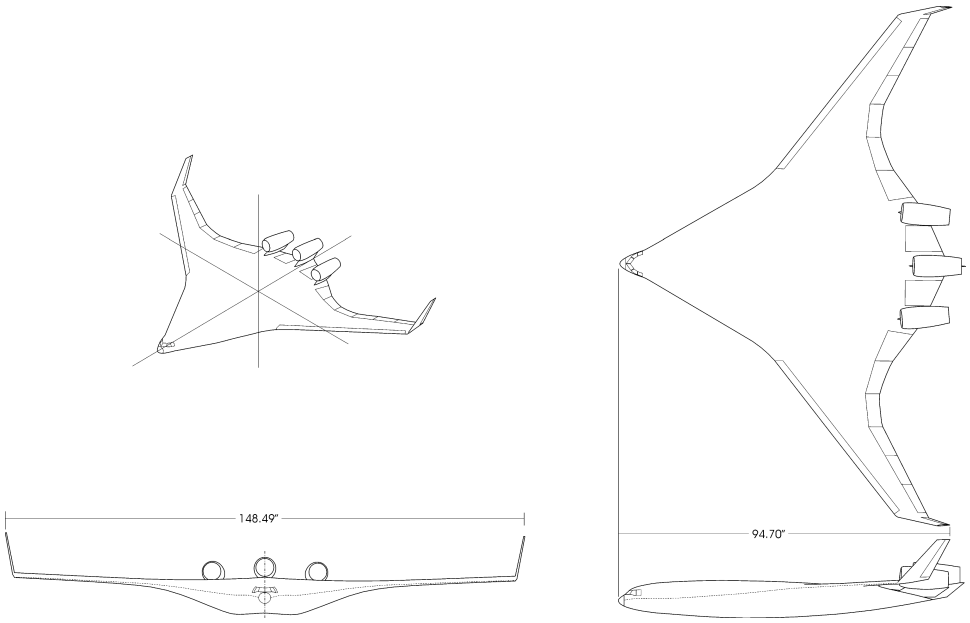

Figure 1. BWB 5 free-flight model

DR	rudder deflection
DSB	speedbrake deflection
HW	hinge-wise, i.e. measured normal to the hinge line
IC	initial condition
SB	speed brake
SW	stream-wise, i.e. along longitudinal axis
TV	thrust vectoring
VME	Versa Module Europa bus
m.a.c.	mean aerodynamic chord

1 Introduction

This document describes the design and implementation of a set of control laws used to support pseudo-free-flight testing of a 5% scale model of a blended-wing-body (BWB) vehicle in the NASA Langley/Old Dominion University Full-Scale Wind Tunnel. A depiction of the model is shown in figure 1.

The model was connected to the facility via an umbilical which provided electrical power, compressed air, and control commands to the on-board sensors, ejectors, and actuators, respectively. On-board sensor measurements were fed back from the model to the external flight control computer via the same umbilical. The flight control computer was located in an adjacent control room which also housed two of three model operators or pilots (see figure 2).

The control laws were required to allow the conditionally stable model to be manually 'flown' by the pilots within the operating wind tunnel in all six degrees-of-freedom at a variety of speeds and angles-of-attack, from zero to maximum coefficient of lift. The control laws had to allow for tunnel start-up which began with the model hanging from an umbilical in the test section as the tunnel fan motors began to rotate the drive fans. In still air the model, supported near its center-of-gravity, hung mostly level but the nose was relatively free to wander from side-to-side.

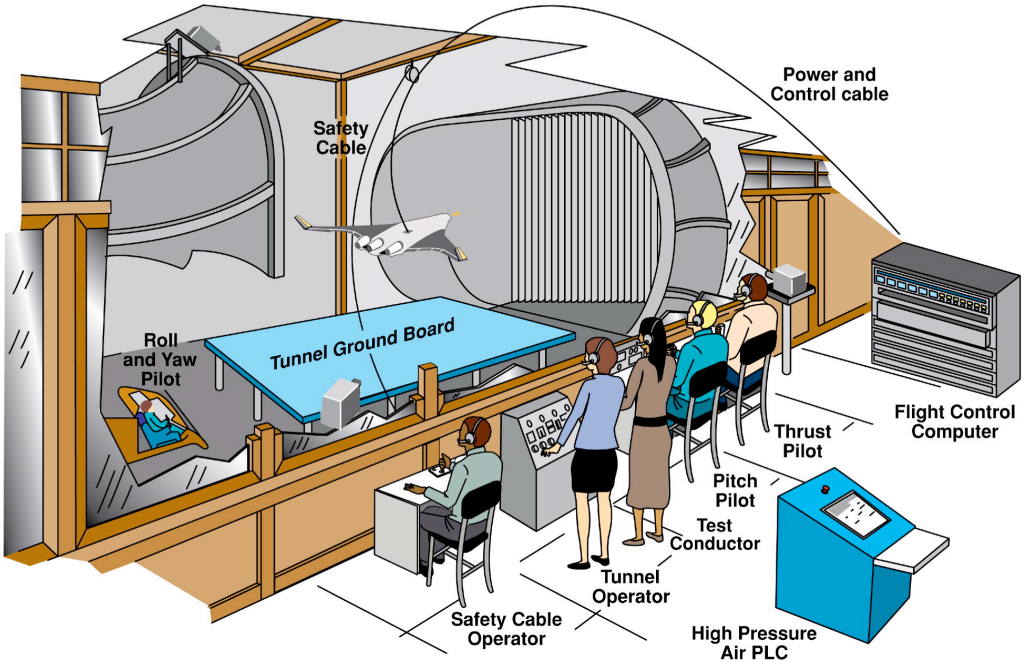

Figure 2. Free-flight testing configuration of the 30x60 Langley Full-Scale Tunnel

To assist in tunnel startup, the center engine nacelle could be commanded to swivel horizontally to provide some control of yaw from thrust vectoring via pressurized air ejectors.

2 Overview

The control laws were designed to provide stability augmentation and compensation for pitch thrust coupling to assist the pilots in the operation and evaluation of the model. The model contained sensors to measure α, β, body rotational rates, nacelle pressures and contained actuators to move the twenty trailing-edge control surfaces and to swivel the center engine nacelle. Several control surfaces were ganged to a single actuator to reduce the number and weight of on-board actuators.

A control law was developed using a preflight aerodynamic model from which linearized state-space models were extracted. The feedback gains were chosen to provide sufficient damping and stability margins in all axes via root locus and Nichols graphical techniques. These control laws were modified and gains adjusted as a result of desktop-simulation experiments and eventually wind-tunnel 'flight' experience. A high-level schematic of the control laws are shown in figure 3.

In addition to stability augmentation the control laws provided a means to allocate pilot commands, in the form of desired pitch, roll and yaw rates, to the various control surfaces. This function was accomplished via control mixing logic with a fixed linear distribution scheme. The mixer was also designed to prevent the clamshell elevon surfaces 6–9 on the outboard end of each wing from being commanded to collide; this bias was increased during these tests to provide additional clamshell extension to improve roll response.

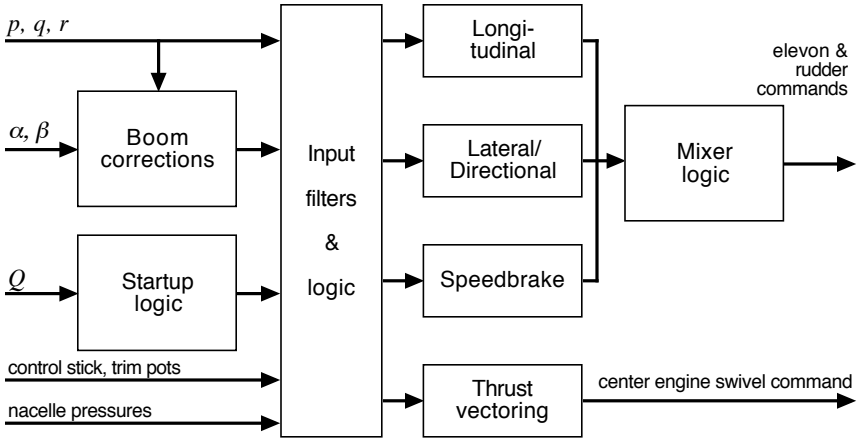

Figure 3. Top-level control law schematic

3 Design requirements

3.1 Vehicle configuration

The 5% BWB model, shown in figure 1, had an 12.4-foot wingspan and weighed approximately 92 lbs depending on configuration. A set of removable full-span leading-edge slats were tested, and a set of ballast weights allowed adjustment of the center of mass from 36% to 40% of the mean aerodynamic chord (m.a.c.).

The umbilical cable was attached to the upper surface of the model roughly above the center of mass and had a swivel connection to reduce the transmission of moments to the vehicle while in flight; the umbilical included a tether to support the vehicle in a level attitude when not flying.

Scaled engine thrust was simulated by use of compressed air exhausting through ejectors mounted in each nacelle. Individual ejector pressures were adjustable via separate valves external to the model; the overall thrust was commanded via a master valve in the control room.

3.1.1 Control surface arrangement

As shown in figure 4, the control surfaces were numbered from the center outward. The inner-most surfaces 1 left and 1 right were driven by separate actuators from the same electrical signal and were thus 'ganged' electrically. Surfaces 2–5 were driven by one actuator per wing. Lower clamshell surfaces 6 & 7 were driven by a single actuator on each wing, as were upper clamshell surfaces 8 & 9. Each vertical rudder had a dedicated actuator as well. The center engine nacelle (engine 2) could be swiveled about the vertical axis by a single actuator.

3.1.2 Control surface allocation

As shown in table 1, four control functions (pitch, roll, yaw and speedbrake) were allocated between the ganged surfaces. The mechanization of this logic is more fully explained in section 5.6 later in this report.

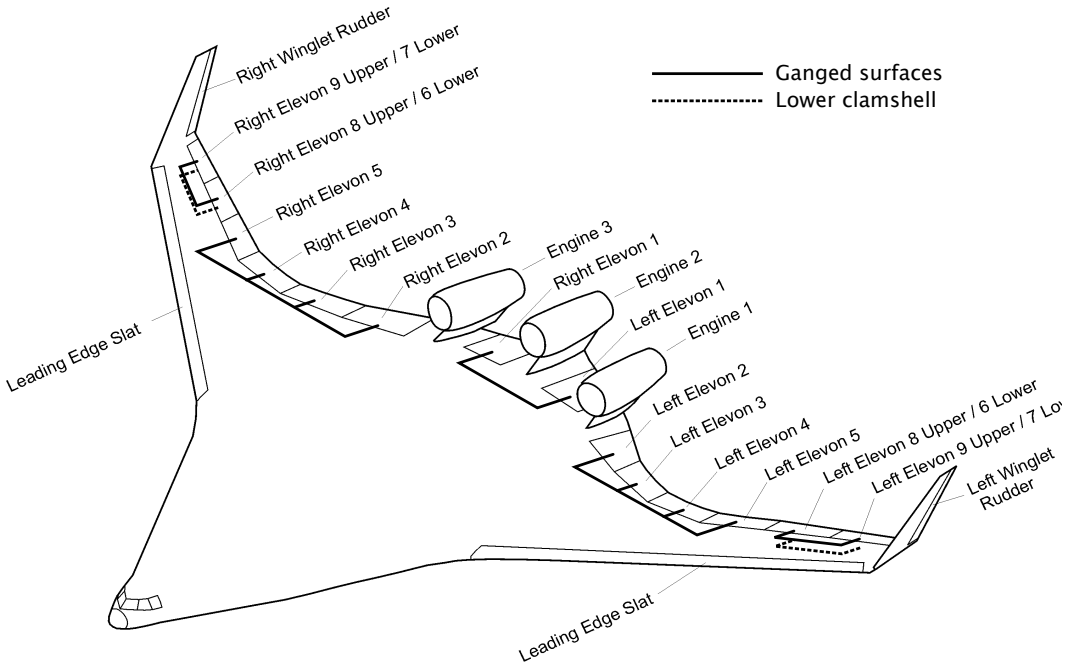

Figure 4. Model actuator ganging and surface numbering scheme

Table 1. Surface allocation of command inputs

Control Function	Elevons 1	Elevons 2–5	Upper clamshell	Lower clamshell	Vertical rudders
Pitch	×	×			
Roll		×	×	×	
Yaw			×	×	×
Speedbrake			×	×	

3.2 Piloting requirements

Piloting was performed by a four-person team: a pitch pilot, who was situated in the upper control room looking across the test section at a profile view of the model; a roll-yaw pilot, who was located below and behind the test section and had a view of the lower rear of the model; a thrust pilot, who modulated thrust via a pressure control valve as shown in figure 2; and a cable operator, also located in the upper control room, who was tasked with positioning the model vertically in the tunnel during start-up prior to 'lift off' and to keep the appropriate amount of slack in the umbilical while airborne to minimize disturbances to the vehicle. The cable operator also worked to keep the model from departing the test section or impacting the test section floor.

A significant piloting challenge of this test configuration was the relatively large time delay in thrust response due to a lengthy run of flexible compressed air hoses from the thrust-pilot-operated control valve in the control room to the ejectors in the model. This was especially an issue for a vehicle with a significant thrust-to-pitch response coupling due to high-mounted engines such as the BWB.

To partially compensate for this effect, measurements of static air pressure levels in the three nacelles were averaged and provided as an input to the control laws, which provided feed-forward compensation into the pitch channel in proportion to changes in nacelle pressures (and thus thrust).

While flying qualities design guidelines are well-established for manned aircraft [MIL-STD1797], little information exists regarding remotely-piloted vehicles, whether being operated from a simulated cockpit with an out-the-window view, from the ground looking at the vehicle in flight, or in this case, observing the vehicle from several external perspectives. Thus, the main requirement of the control design was to provide stability in all three rotational axes with adequate damping for all modes in the typical pilot's bandwidth. Another requirement was to provide compensation for coupling between thrust changes and pitch response and to provide reasonable coordination between the roll and yaw response to minimize sideslip while maneuvering. Adequate gain and phase margins needed to be maintained to insure a design robust to differences between expected and actual vehicle aerodynamics.

4 Implementation

4.1 Development tools

The control laws were developed using Matlab® Simulink® release 14 service pack 2 (version 7.0.4) and the equivalent C source code was generated using the Real-Time Workshop Embedded Coder® (version 6.2).

4.2 Input signal conditioning

4.2.1 Analog filtering

All input signals coming from sensors in the model were passed through an analog filter card in the flight control computer. The filter was a three-pole 40 Hz Butterworth filter. These filtered signals were then converted to digital measurements for use by the control laws. Further filtering and limiting of these digital signals are described in this report.

In normal operation the ejector pressure measurements from all three nacelles averaged to form a single, averaged, ejector pressure measurement which was provided to the control laws. When asymmetric thrust tests were conducted with the flow through one of the nacelles reduced, the control system operator could remove that signal from calculation of the average, ahead of the control law digital filtering.

4.2.2 Digital filtering

In addition to the analog filtering performed by the flight control computer signal acquisition hardware, the control laws included digital limits and filters described here.

Figure 5 depicts an overview of the signal conditioning for the angle-of-attack and sideslip measurement signals. These originate from an alpha-beta 'bird' sensor at the end of a 8" probe mounted on the nose of the BWB model. The electrical voltage from these sensors was converted into scaled engineering units (deflection angle in degrees) based on preflight, wind-off, calibrations of the probe using software that was not part of these control laws. The angle of attack measurement was then corrected for up-wash and position error as shown in the diagram using a linearly-interpolated one-dimensional function table.

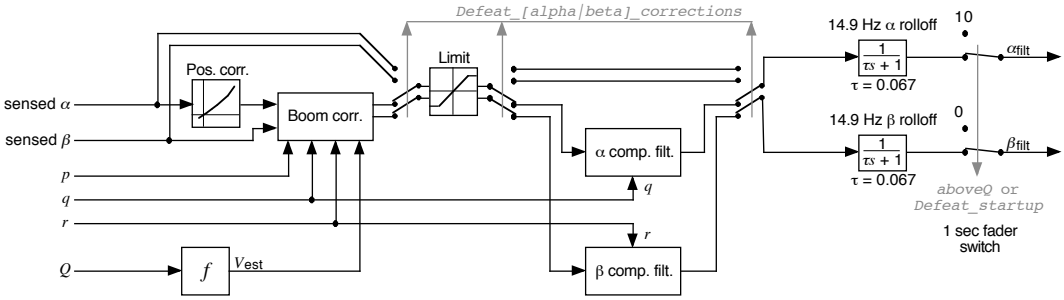

Figure 5. Simplified α and β filtering strategy

Both sensed α and β were then corrected for errors induced by rotational motion of the vehicle about the center of gravity. This moment arm or boom correction required an estimate of velocity, which came from a measurement of tunnel dynamic pressure Q.

To reduce high-frequency noise, complementary filters were used for both angle-of-attack and sideslip signals. Filtered body pitch-rate q and negative body roll-rate $-r$ were used as estimates for $\dot{\alpha}$ and $\dot{\beta}$, respectively. The cross-over frequency of the complementary filters was set at 5 Hz after reviewing time histories of static tunnel runs and estimating the bandwidth of the sensors.

A final selection switch was applied to angle-of-attack and sideslip signals to avoid any startup-transient at low tunnel speeds when the alpha-beta sensor might be unreliable. While the wind tunnel dynamic pressure remained below a reasonable value (indicated by `aboveQ` *false*), the downstream control laws were provided with fixed values of 10 and 0 degrees, respectively, for α_{filt} and β_{filt}. As soon as measured tunnel dynamic pressure exceeded a certain value, `aboveQ` was latched *true* and the filtered values of angle-of-attack and sideslip were passed to the control laws through a one-second fader switch. The latch of `aboveQ` ensured that measured α and β were used, regardless of subsequent changes in tunnel dynamic pressure.

A bypass discrete, `Defeat_startup`, provided the control operator the ability to send alpha-beta sensor measurements directly to the control law regardless of tunnel pressure; this was provided for preflight checkout of the control system.

Other feedback signals, including roll, pitch and yaw rates and engine nacelle pressure measurements, were digitally filtered with a first-order lag filter. All feedback signals were limited ahead of any filtering.

Table 2 gives the values for the input signal limiters and filter characteristics.

Table 2. Input signal limits and filtering characteristics

Signal	Units	Limits	Roll-off (Hz)
α	deg	0 to 40	14.9
β	deg	± 20	14.9
p, q, r	deg/s	± 90	14.9
Avg. ejector pressures	lb/in^2	0 to 25	2.0
Inceptor positions	- -	± 1	- -

4.3 Control design method

Initial control law architecture and gain values were based on a pre-flight aerodynamics model of the full-scale aircraft, scaled to the 5% dynamically-scaled free-flight wind tunnel model. Two aerodynamic configurations (with slats extended or retracted) and two center-of-gravity positions (36.39% and 40.13% m.a.c.) were to be tested.

From the non-linear simulation, linear models of the rigid, unaugmented vehicle in trimmed conditions (where angle of attack, throttle setting, and elevator position were set to achieve unaccelerated flight at a given dynamic pressure) and untrimmed conditions (where dynamic pressure was perturbed from trim) were generated using a central-difference algorithm. This bare airframe plant model was then augmented with second-order actuator models, Butterworth signal conditioning filters, and the alpha-beta complementary filters to form an augmented plant model. This augmented plant model was then used to set feedback gains to provide adequate damping (using root-locus techniques) and robustness (using a Nichols diagram), in an iterative fashion. The vehicle was assumed to be rigid, i.e. no structural modes were modeled.

The non-linear aerodynamics model and resulting candidate control laws were then autocoded into C and used in a desktop pseudo-real-time simulation environment based on LaRCsim [Jackson95] in which both unconstrained and tethered flight was replicated with a conventional joystick hand controller to determine approximate handling qualities and to confirm appropriate control law operation.

This process concentrated on the aft center-of-gravity (40.13%), slats extended, configuration which appeared to be the worst case from a stability standpoint. Minor gain changes were made for the forward center-of-gravity (36.39%), slats extended configuration. No control law architectural changes were required for tunnel flights with slats retracted but some gain changes were required as described in the Results section later in this report.

4.4 Control law overview

An overview of the control laws will be presented in this section. In section 5 the complete set of control laws will be presented.

4.4.1 Longitudinal axis

Figure 6 presents a simplified diagram of the longitudinal-axis control law.

As shown in figure 6, pitch pilot commands in the form of pitch control stick deflections ('pitch stick') and pitch trim settings were multiplied by `long_ff_gain` and `PTRIM_gain`, respectively; these signals were then added together and scaled by a fixed gain of -5 before being added to the feedback signals.

Feedbacks to the longitudinal control law were pitch rate, angle of attack, and average nacelle ejector pressure. These feedbacks provided damping, stabilization and thrust pitch

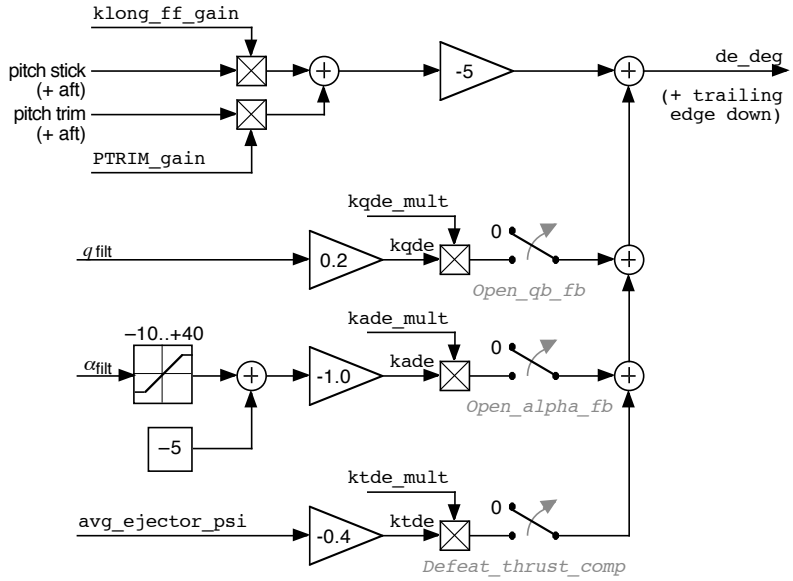

Figure 6. Simplified longitudinal control laws

compensation, respectively; the values for the feedback gains were mechanized as functions of filtered angle of attack.

The controller provided a means to add multipliers to each of the three feedback paths as well as a means to disable each feedback path independently, as shown in figure 6.

4.4.2 Lateral-directional axis

Figure 7 gives a simplified diagram of the lateral-directional-axis control law.

As shown in figure 7, the lateral control law accepted roll pilot commands ('roll stick') and roll trim inputs as well as yaw trim inputs. No direct yaw, or rudder pedal, input was used.

In the lateral channel, roll stick input was multiplied by an adjustable gain (`lat_ff_gain`) and then by a fixed gain of +60 forming a commanded roll rate; this commanded roll rate was then subtracted from filtered measured roll rate p_{filt} to form a roll-rate error. This error signal was multiplied by a non-linear gain, `kpda`, which was a function of filtered angle of attack a_{filt} as well as an optional adjustable gain, `kpda_mult`, to form an aileron command intended to reduce the roll-rate error. The roll trim signal was used to allow a nulling adjustment to this command.

In the yaw channel, filtered body yaw rate and sideslip measurements were multiplied by two nonlinear gains, `krdr` and `kbetadr` respectively, and summed along with the yaw trim potentiometer signal. To this sum was added a portion of the aileron command, scaled by an aileron-to-rudder interconnect (ARI) gain, to form the rudder command signal.

This ARI path could be defeated, as could roll, yaw, and sideslip feedbacks, as shown in figure 7, by the roll pilot using switches provided at his control station.

An optional yaw channel output was a command to swivel the center engine nacelle from left to right; this was intended to provide limited yaw control at low tunnel speeds. This output was formed by multiplying the rudder command signal `dr_deg` by gain `TV_dr_gain`, in the case that the ARI path was engaged; when ARI was not engaged, the roll stick signal

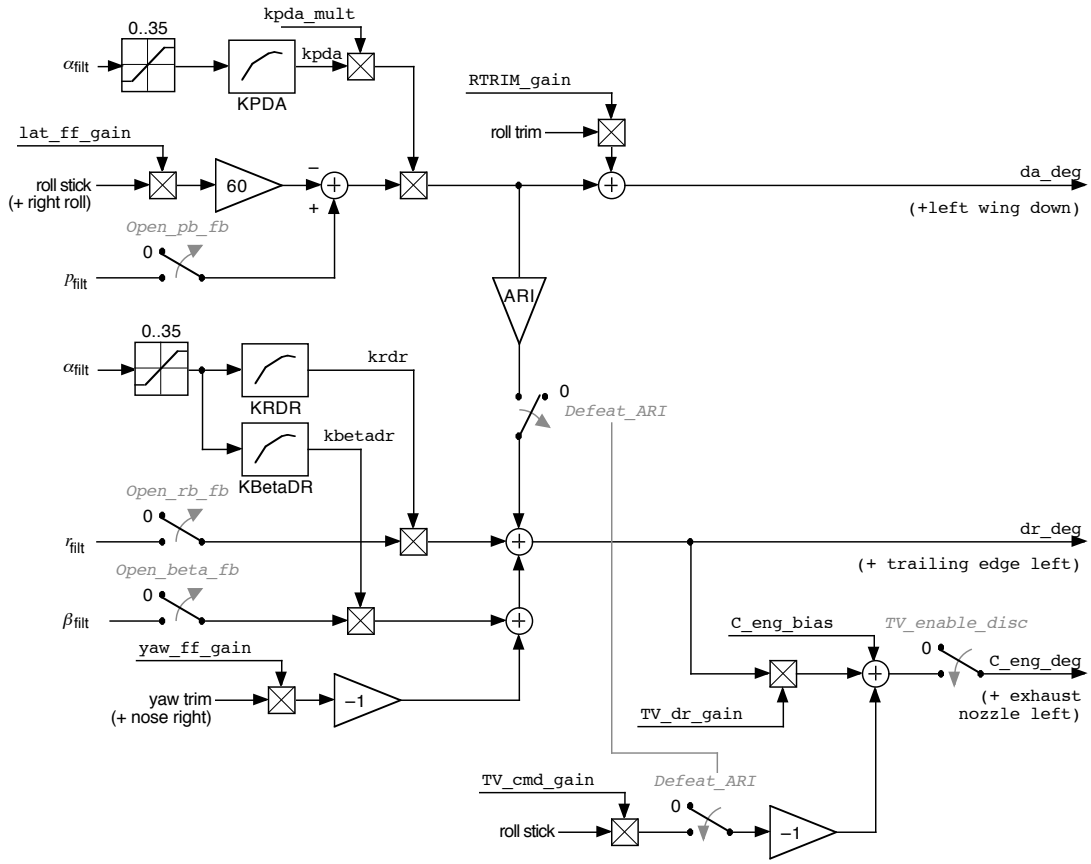

Figure 7. Simplified lateral-directional control laws

drove the engine swivel directly through a gain (TV_cmd_gain) as shown in the figure.

4.5 Control law inputs

The control law allowed for 57 different input signals, including pilot control inputs, test operator inputs, and feedback signals from sensors on the model as well as tunnel dynamic pressure. The various inputs and nominal values are given in this section.

The pitch pilot control station included two analog inputs and four discrete inputs, as shown in table 3.

Table 3. Control law inputs from the pitch pilot's control station

Name	Signal Description	Range	Sense
Long_cmd_norm	Pitch stick position	−1 to +1	+aft
PTRIM	Pitch trim position	−1 to +1	+aft
Defeat_thrust_comp	Turn off thrust compensation	0 or 1	1=*true*
Defeat_alpha_corr	Defeat alpha boom correction	0 or 1	1=*true*
Open_alpha_fb	Remove alpha feedback	0 or 1	1=*true*
Open_qb_fb	Remove pitch rate feedback	0 or 1	1=*true*

The primary pitch control input was the pitch stick, which was mounted transverse relative to the pilot in the control room so that a right-to-left motion of the stick resulted in a pitch-up command; this corresponded with the pitch pilot's profile view of the model which was normally pointed with the nose of the model to the right.

The roll/yaw pilot's control station included four analog and six discrete switches, as shown in table 4.

Table 4. Control law inputs from the roll pilot's control station

Name	Signal Description	Range	Sense
Lat_cmd_norm	Roll stick position	−1 to +1	+right wing down
RTRIM	Roll trim position	−1 to +1	+right wing down
YTRIM	Yaw trim position	−1 to +1	+nose right
C_Eng_bias	Engine swivel nulling command	−1 to +1	+nozzle right
TV_enable_disc	Thrust vector enable switch	0 or 1	1=*true*
Defeat_beta_corr	Defeat beta boom correction	0 or 1	1=*true*
Defeat_ARI	Defeat aileron-to-rudder interconnect	0 or 1	1=*true*
Open_beta_fb	Remove beta feedback	0 or 1	1=*true*
Open_pb_fb	Remove roll rate feedback	0 or 1	1=*true*
Open_rb_fb	Remove yaw rate feedback	0 or 1	1=*true*

The primary roll flight control was the roll stick position, augmented by the roll trim knob. A yaw trim knob was also provided, as well as a center-engine-nacelle centering knob. Defeat switches for most lateral/directional feedbacks and a thrust-vector enable switch were provide as shown in the table. No direct yaw control was provided.

Six feedback signals from the model are described in table 5, along with a single input from the tunnel instrumentation giving tunnel dynamic pressure.

Table 5. Control law feedback signals from model sensors

Name	Signal Description	Units	Sense
avg_ejector_psi	Average ejector pressure	lb/in^2	- -
PB_dps	Body-axis roll rate (p)	deg/s	+right wing down
QB_dps	Body-axis pitch rate (q)	deg/s	+nose up
RB_dps	Body-axis yaw rate (r)	deg/s	+nose right
Sensed_alpha_deg	Angle-of-attack (α)	deg	+nose up
Sensed_beta_deg	Angle-of-sideslip (β)	deg	+from right
Tunnel_Qbar_psf	Tunnel dynamic pressure (Q)	lb/ft^2	- -

Three body-rate angular rate measurements were provided by gyros internal to the model; flow angularity relative to the model was sensed by an alpha/beta 'bird' on a boom mounted on the nose.

The tunnel provided a measurement of freestream dynamic pressure to indicate tunnel speed; this was used by the control law to estimate vehicle velocity relative to freestream by assuming the model to have little motion relative to the tunnel.

The control system operator had a number of discrete and floating-point value settings that could be changed at run-time to affect the operation of the control law; these are given in tables 6 and 7.

Table 6. Control law discrete inputs from control system operator

Name	Signal Description	Nominal Value	Sense
Claw_reset	Control law reset	0	$1 \rightarrow 0$ = reset
Fixed_gains	Select fixed gains	0	1=fixed gains
Pitch_nonlin	Pitch stick nonlinearity adjustment	0	0=linear
Defeat_startup	Go straight to operate mode	0	1=defeat
Defeat_boom_corr	Turn off boom corrections	0	1=defeat

Provisions for six additional inputs are shown in the detailed control diagrams (starting with figure 8) that were not implemented in the control law or not exercised in these tests. These unused inputs are listed in table 8. The speedbrake toggle was implemented but was not exercised; the other five inputs were not connected logically to any control law element.

In addition to these unused inputs, the model also contained an accelerometer in each axis whose measurements were available for data recording; the control law described here did not use accelerometer feedback.

4.6 Control law outputs

The control law provided a number of output parameters which included intermediate calculations or test-points for debugging purposes. The primary outputs, however, were the ten control actuator commands which are presented in table 9.

4.7 Flight control computer

The control law was executed on a 1.26 GHz Pentium III processor-based single-board computer in a Versa Module Europa (VME) chassis running the Wind River® VxWorks®5.4

Table 7. Control law gain value inputs from control system operator

Name	Gain description	Nominal Value	Units
Kpda_mult	Roll error-to-aileron feedback multiplier	varied	deg/deg/s
Krdr_mult	Yaw-to-rudder feedback multiplier	varied	deg/deg/s
Kbdr_mult	Beta-to-rudder feedback multiplier	1.0	deg/deg
Kqde_mult	Pitch rate to elevator feedback multiplier	varied	deg/deg/s
Kade_mult	Alpha to elevator feedback multiplier	varied	deg/deg
Ktde_mult	Thrust to elevator feedback multiplier	varied	deg/lb/in^2
roll_fb_mult	Roll to aileron feedback multiplier	1.0	- -
Kpda_test	Fixed gain for roll rate to aileron	0.053	deg/deg/s
Krdr_test	Fixed gain for yaw rate to rudder	0.650	deg/deg/s
Kbdr_test	Fixed gain for beta to rudder	-1.355	deg/deg
Kqde_test	Fixed gain for pitch rate to elev	0.200	deg/deg/s
Kade_test	Fixed gain for alpha to elev	0.0	deg/deg
Ktde_test	Fixed gain for thrust to elev	-4.0	deg/lb/in^2
PTRIM_gain	Pitch channel trim gain	3.0	- -
PTRIM_bias	Pitch trim bias value	0.0	deg
RTRIM_gain	Roll channel trim gain	-15.0	- -
long_ff_gain	Longitudinal feedforward gain	varied	- -
lat_ff_gain	Lateral feedforward gain	varied	- -
yaw_ff_gain	Directional feedforward gain	20.0	- -
ma_desired	Target M_α stability parameter value	0.0	ft-lb/deg
ARI_gain	Aileron-to-rudder interconnect gain	varied	deg/deg
TV_cmd_gain	Engine swivel command gain	2.0	deg
TV_dr_gain	Engine swivel rudder gain	0.1	deg/deg

Table 8. Unused control law inputs

Name	Signal Description	Nominal Value	Sense
DSB_toggle	Speedbrake extend/hold/retract switch	0	$\begin{cases} \text{retract} & < 0 \\ \text{hold} & = 0 \\ \text{extend} & > 0 \end{cases}$
Phi_deg	Roll attitude, deg	not used	
Theta_deg	Pitch attitude, deg	not used	
Yaw_cmd_norm	Yaw command input	not used	
Pitch_hold_on	Pitch attitude hold switch	not used	
Roll_hold_on	Roll attitude hold switch	not used	

Table 9. Control law output commands (all units in deg measured about hinge line)

Name	Signal Description	Sense
`elev1`	Elevon 1 position	+trailing edge down
`elev25L`	Left elevon 2–5 position	+trailing edge down
`elev67L`	Left lower elevon 6–7 position	+trailing edge down
`elev89L`	Left upper elevon 8–9 position	+trailing edge down
`elev25R`	Right elevon 2–5 position	+trailing edge down
`elev67R`	Right lower elevon 6–7 position	+trailing edge down
`elev89R`	Right upper elevon 8–9 position	+trailing edge down
`rudderL`	Left rudder position	+trailing edge left
`rudderR`	Right rudder position	+trailing edge left

operating system; the control law was executed 200 times per second, yielding a frame time T of 5 milliseconds.

5 Detailed control law architecture

A more detailed diagram of the outermost-level arrangement of the control law structure is shown in figure 8; this is an elaboration of the simplified overview previously depicted in figure 3. This diagram and the ones that follow were generated directly from the Matlab® Simulink® design tool cited earlier and correspond to control law version 1.07a, revision 490.

In this design, a boom-corrections block preceded the control law block; the outputs of the control law block (consisting of generic pitch, roll, yaw commands labeled elevator, aileron and rudder commands) served as inputs to the mixer logic block. Also shown on this diagram are run-time adjustable inputs to parts of the control law and test input and output signals.

5.1 Utility blocks

The block diagrams described in this section were used in several places in the control system; they are described here to reduce duplication.

5.1.1 Lag/Roll-off Filter

The lag/roll-off filter block is shown in figure 9.

Copies of this filter were used several times in the control system, primarily in the input signal conditioning block but also in the tunnel start logic block. It implemented a first-order lag filter with a transfer function of

$$\frac{y}{u} = \frac{1}{\tau s + 1}$$

discretized via the Tustin transformation

$$s \equiv \frac{2}{T}\frac{(z-1)}{(z+1)} \tag{1}$$

to a digital filter with transfer function of

$$y_n = \frac{1}{2\tau + T}[T(u_n + u_{n-1}) + (2\tau - T)y_{n-1}]$$

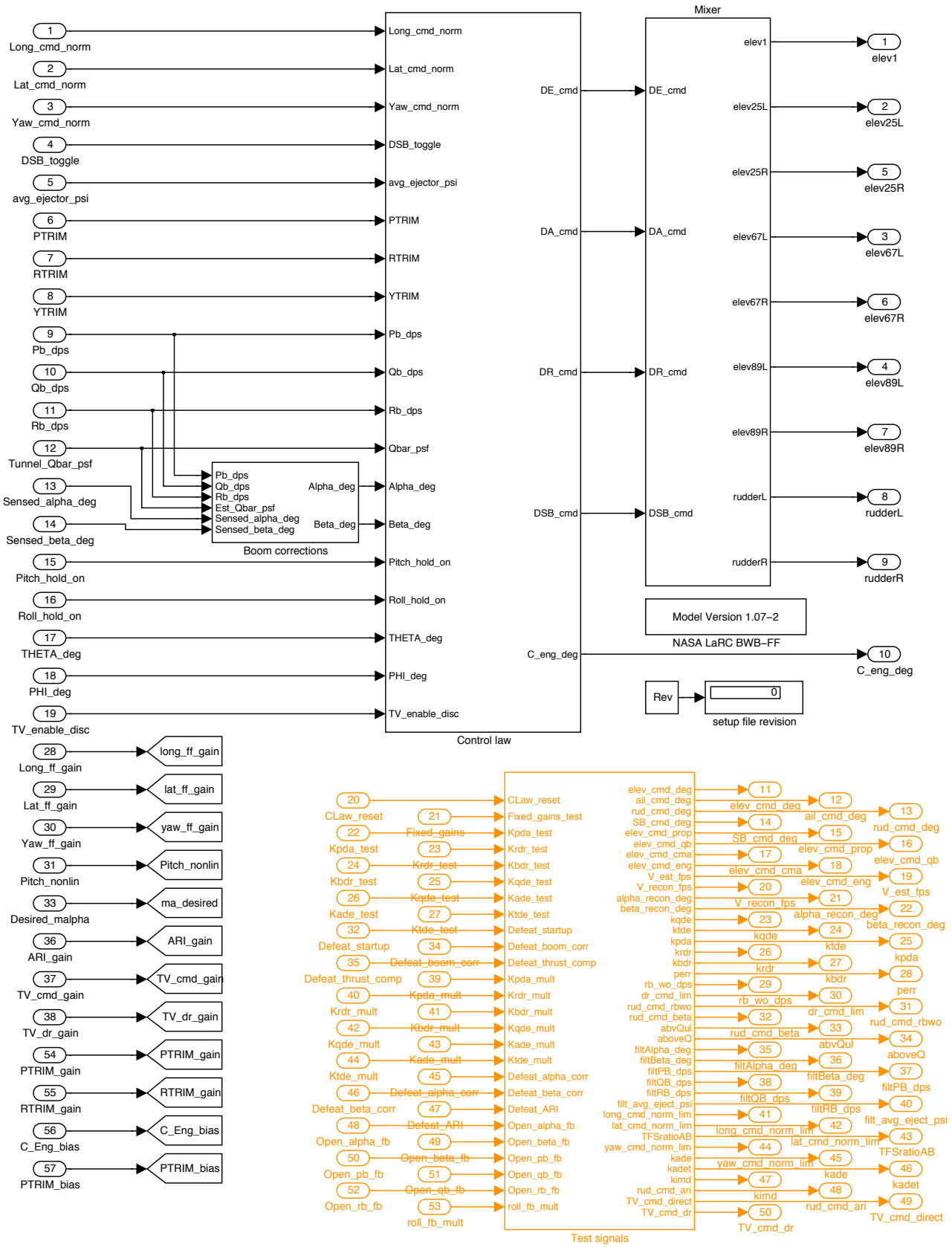

Figure 8. Top-level control law structure

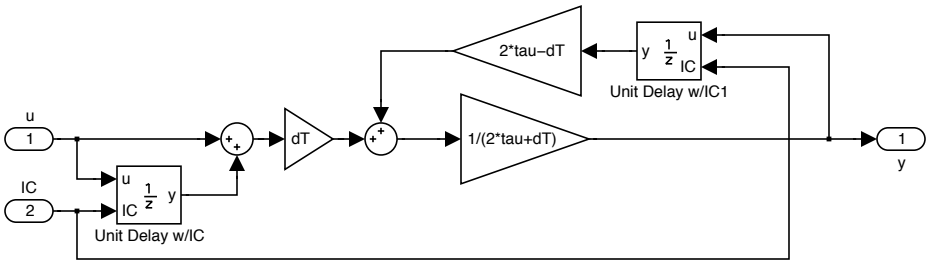

Figure 9. Discrete first-order lag filter implementation

where τ is the time constant of the filter and T is the incremental time step size of the digital control system. The two states of this filter (u_n and y_n) required initialization, so a unit delay block with initial condition, described below, was devised to provide this capability. The value for τ was chosen to match the inverse of the desired roll-off frequency as shown in table 10.

Table 10. First-order lag/roll-off filter applications

Filtered signal	Application	Roll-off, Hz	τ, s
α, β	Input conditioning	5	0.2
p, q, r	Input conditioning	14.9	0.067
`avg_ejector_psi`	Input conditioning	2	0.5
Q	Tunnel start logic	2	0.5

5.1.2 Unit Delay with initial condition

The unit delay block with a specified initial condition is shown in figure 10.

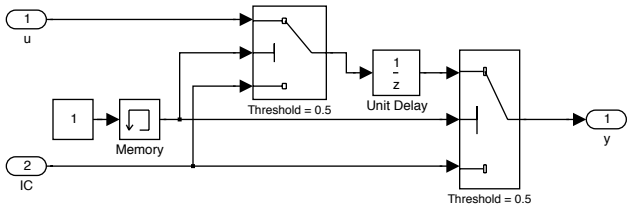

Figure 10. Unit delay with initial condition block

This block provided an initializable one-cycle delay function. On the first pass, the output of the memory block was 0, so the input to the unit delay block as well as the output value was set to the initial condition 'IC' input value. On subsequent evaluations,

the memory output had a constant value of 1, causing the switches to select their upper inputs and thus the block performed as a normal unit delay.

5.1.3 Complementary filter

There were two complementary filters used in signal conditioning, one for angle-of-attack and one for angle-of-sideslip measurements. This filter was employed to blend position (U) and rate ($\dot{U}$) information for one signal from two different sensors to reduce high-frequency noise and steady-state bias. In this BWB free-flight tunnel application, angle-of-attack (α) and pitch rate (q) information were blended to obtain a cleaner estimated angle-of-attack; in like manner, angle-of-sideslip (β) was blended with negative yaw rate ($-r$) for a better estimate of angle-of-sideslip.

The implementation is shown in figure 11.

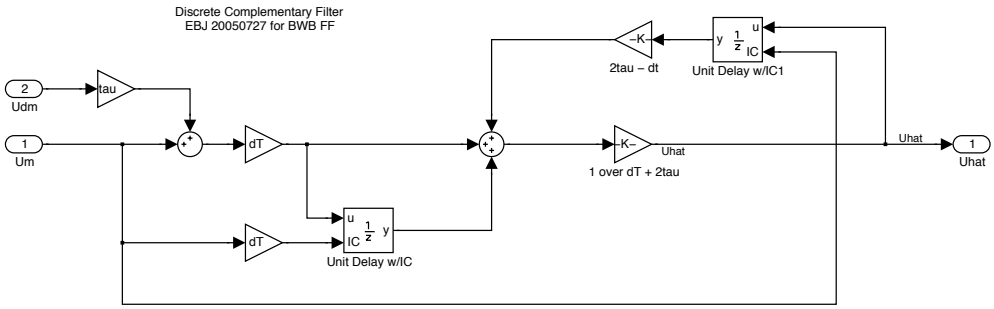

Figure 11. Complementary filter discrete implementation

This was a digital implementation of the continuous filter

$$\hat{U} = \frac{\tau}{\tau s + 1}\dot{U}_{sensed} + \frac{1}{\tau s + 1}U_{sensed}$$

where

U_{sensed} is the measured signal (either α or β)
$\dot{U}_{sensed}$ is the measured derivative of the signal (either q or $-r$)
$\hat{U}$ is the estimated value of the signal (either $\hat{\alpha}$ or $\hat{\beta}$)
τ is the time constant of the filter
s is the Laplace operator

using the Tustin convolution (equation 1).

5.1.4 Apply gain and kill switch

This block, shown in figure 12, had three inputs: an input signal `in`, a gain value `gain`, and a discrete kill input `off`. If `off` was *true* (> 0.5), the output of this block was zero; otherwise, the output was the product of `in` times `gain`.

This block was used several places to provide both a run-time adjustable gain and a run-time disconnect switch for a feedback signal.

5.1.5 Kill switch

This block, shown in figure 13, was identical to the apply gain and kill switch block except with fixed unity gain and was used in several places in the control law.

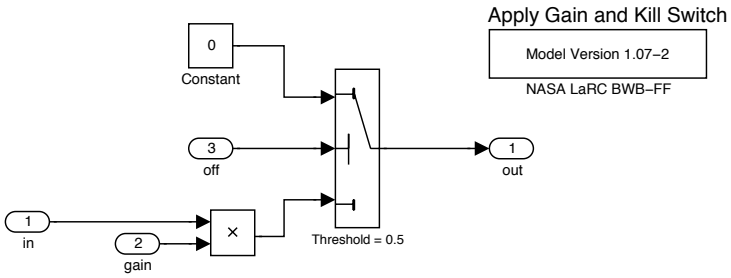

Figure 12. Apply gain and kill switch block

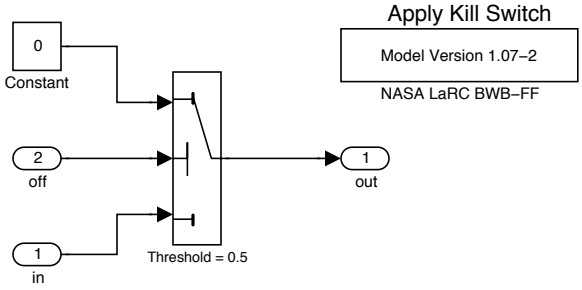

Figure 13. Kill switch block

5.2 Boom position correction logic

The boom correction logic is shown in figure 14.

This block preceded the control law block and to provided corrections for the effects of rotary motion of the vehicle which, due to the location of the angle-of-attack and angle-of-sideslip sensors some distance from the center of mass, induced errors in measurements of flow angularity. These sensors were mounted on an 8" probe extending from the nose of the vehicle.

Prior to correcting for boom moment arm effects, a non-linear one-dimensional function table provided a position error/up-wash correction to the statically calibrated (wind-off) angle-of-attack (α) measurement. The values used during the latter part of these tests is given in table 11.

Table 11. Up-wash and position corrections

α_{sensed}, deg	corrected α, deg
-15	-7.5
0	0
10	4
16	10
45	40

The moment arm correction accounts for the $\vec{\omega} \times \vec{r}$ cross product term; this was done by forming the body rotation vector $\vec{\omega}$ from p_{filt}, q_{filt}, and r_{filt} and forming a cross-product

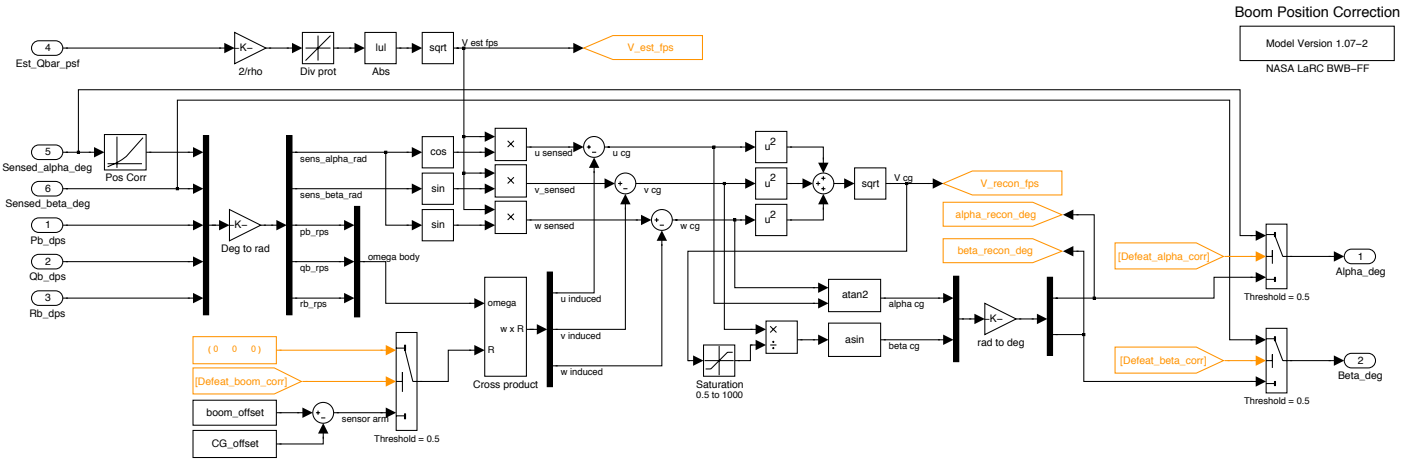

Figure 14. Boom position correction logic

(described below) between $\vec{\omega}$ and the offset vector of the sensor boom location relative to the vehicle's center of mass. The resulting induced body-axis velocities $u_{induced}$, $v_{induced}$ and $w_{induced}$ were subtracted from the uncorrected estimates of these terms (u_{sensed}, v_{sensed} and w_{sensed} which were derived from estimated velocity V and sensed α and β) to form corrected estimates of body-axis velocities at the center of mass (u_{cg}, v_{cg} and w_{cg}).

Corrected α_{cg} and β_{cg} were then constructed from this estimated vector magnitude V_{cg} via a protected division, arc tan and arcsine operations.

If discretes `Defeat_alpha_corr` and/or `Defeat_beta_corr` were greater than 0.5 the calibrated sensed α and β were used in place of corrected α_{cg} and β_{cg}, respectively.

5.2.1 Cross-product block

This block, shown in figure 15, was used in the boom corrections logic to perform a cross-product operation on two three-element vectors representing the body rotation vector $\vec{\omega}$ and the boom position offset vector $\vec{r}$ to form

$$\vec{\omega} \times \vec{r} = \begin{vmatrix} \vec{i} & \vec{j} & \vec{k} \\ p & q & r \\ r_x & r_y & r_z \end{vmatrix}$$

5.3 Inner loop control law

Figure 16 shows the components of the inner-loop feedback control law.

Inputs to the control law were pilot inceptor inputs, speedbrake extend/retract discrete, feedback sensor inputs, and a thrust-vectoring-enabled discrete. Two additional discrete inputs, pitch hold and roll hold, were to support a planned outer-loop function that was not implemented.

Outputs from the control law, commands to virtual elevator, rudder, aileron and speedbrake surfaces, were directed to the mixer block; a fifth output commanded center engine deflection for thrust vectoring, was used in tunnel start-up and asymmetric thrust testing.

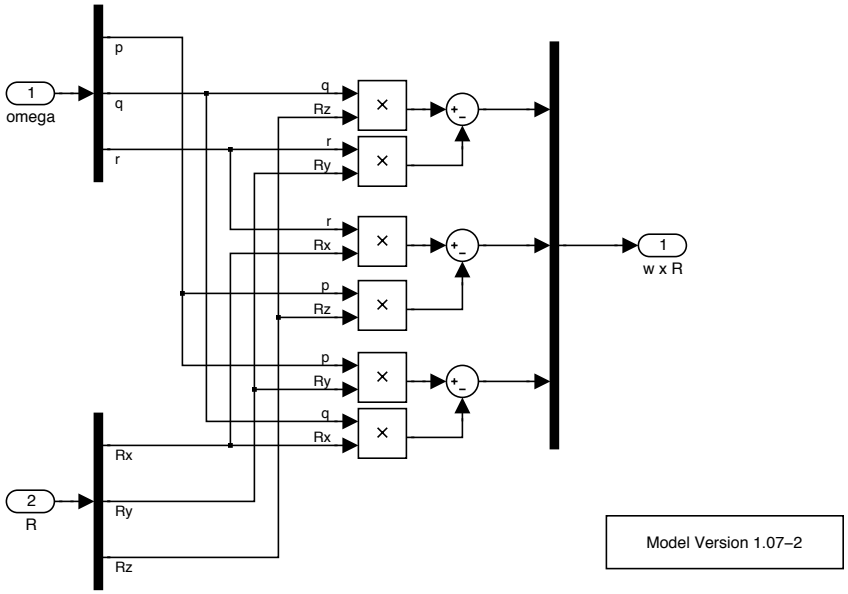

Figure 15. Cross-product block

5.3.1 Input conditioning and signal selection

Figure 17 depicts the input signal conditioning and selection algorithm used by the inner control law.

This algorithm limited, filtered, and selected feedback signals from on-board sensors to provide inputs to the inner loop control law. It included a transient-free switch block to avoid abrupt changes in α and β as the tunnel started up, as described next.

The transient-free switch block contained logic to provide a transient-free selection for both α and β feedback as shown in figure 18. This logic linearly switched the output from input `A` to input `B` over `TFStime` to avoid abrupt changes in the value of the output signal. Another input, `selAnotB`, forced the immediate selection of `A` as the output signal with no transient protection; this was included to support checkout of the model before flight.

5.4 Longitudinal control law

The longitudinal control law, shown in figure 19, accepted the pitch pilot input `Long_cmd_norm` and passed it through a variable shaper block; in these tests, the stick shape was strictly linear (that is, the output was equal to the input) so the shaper block did not distort the pitch pilot input (`Pitch_nonlin` was 0). A variable scaling `long_ff_gain` was then applied to the input, followed by the pitch trim analog input, `PTRIM`, with appropriate scaling. The combined stick plus trim command passed through another gain, `klong_ff`, before being summed with feedback signals to form the elevator command `de_deg`. `klong_ff` was fixed at -5.0 for the whole test series.

Feedback signals consisted of three paths: pitch rate feedback, an angle-of-attack compensation, and thrust compensation.

The pitch rate feedback used filtered body-axis pitch rate `Qb_dps` scaled by a gain that could be scheduled on angle-of-attack, `Kqde`. This feedback could be defeated if `Open_qb_fb` was *true*, which was controlled by a switch at the pitch pilot's control station. For this test series, `Kqde` was a constant value of 0.2 regardless of the value of `Alpha_deg`.

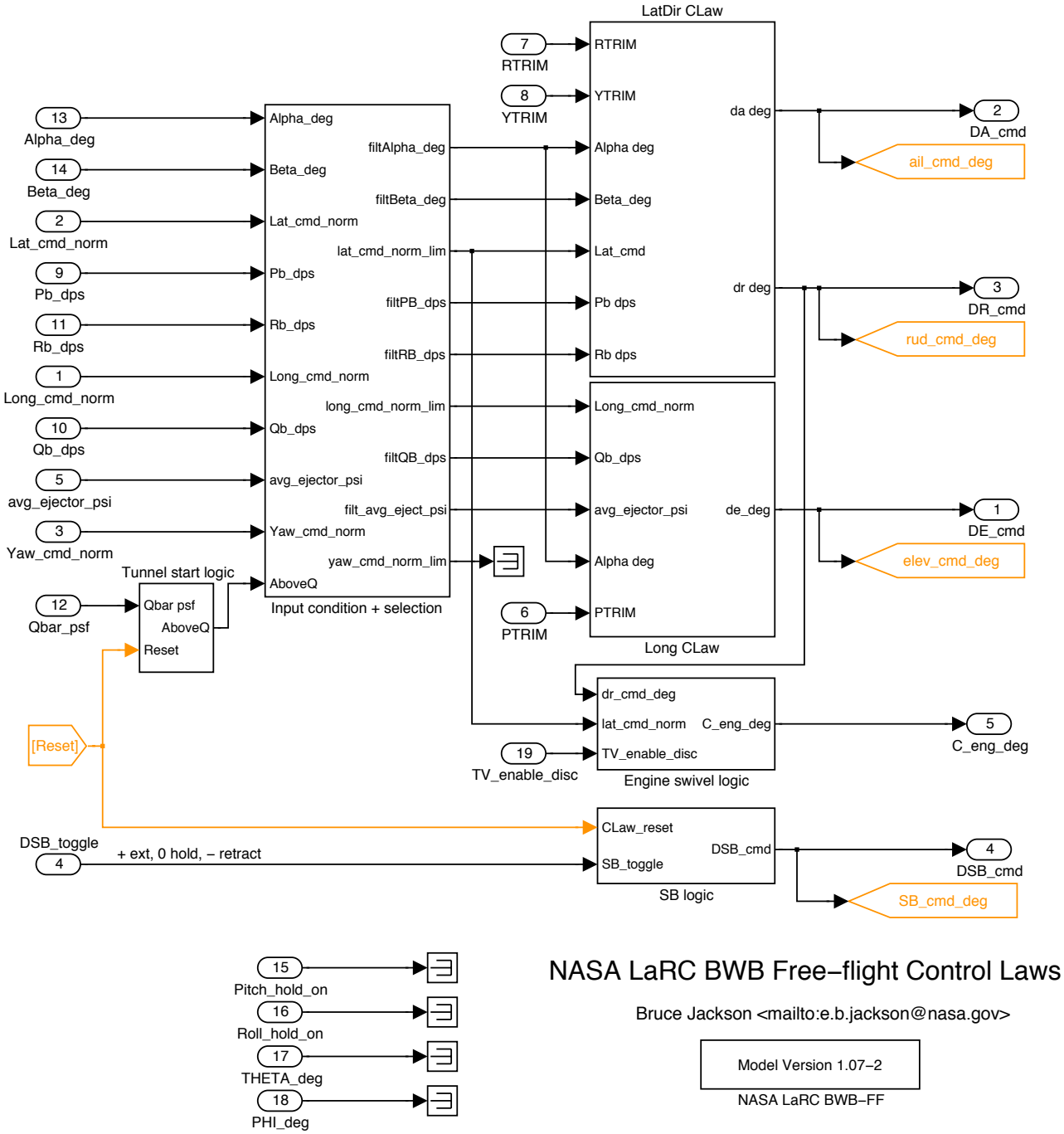

Figure 16. Inner-loop control law ("Control law" block)

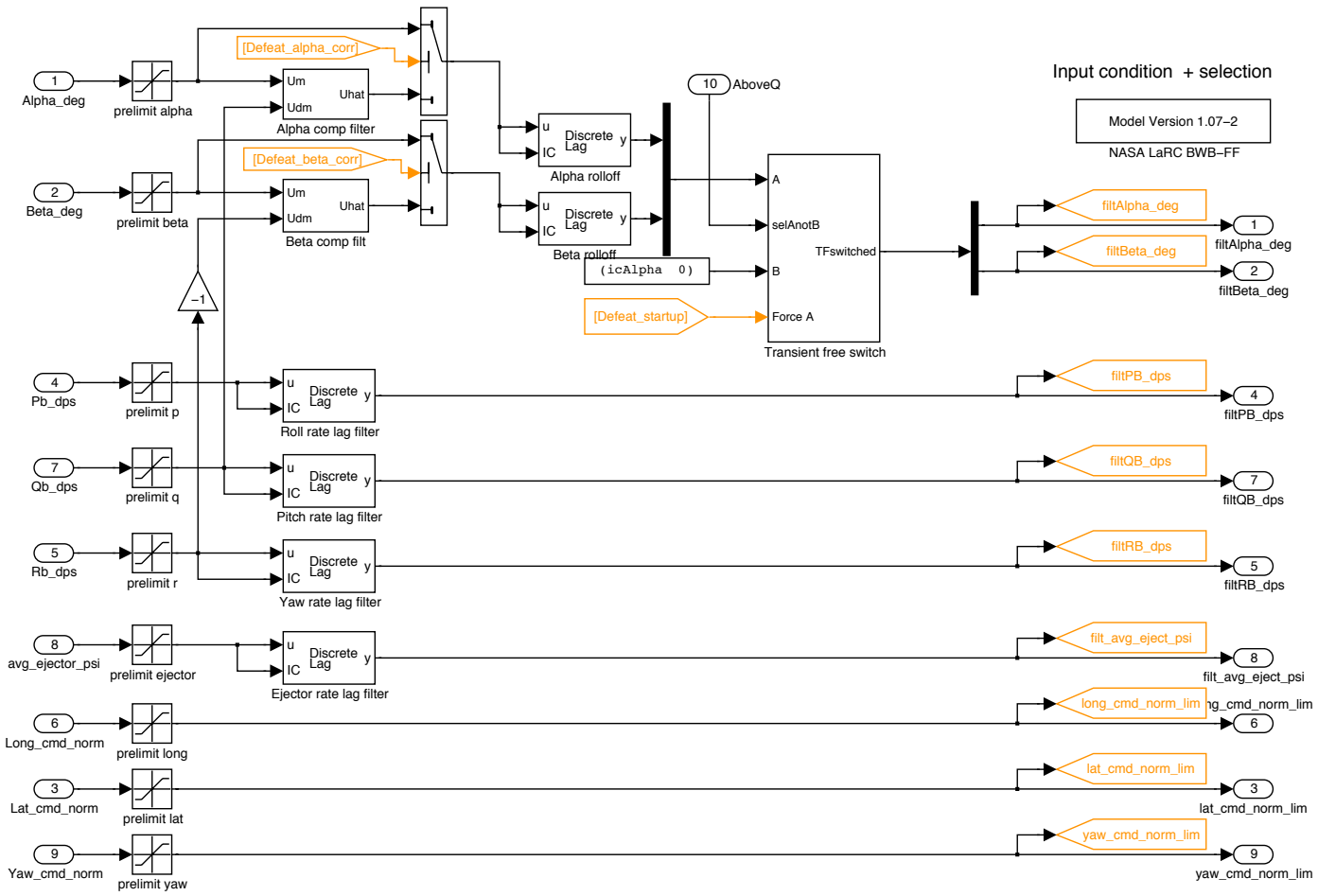

Figure 17. Input condition and selection block ("Input condition + selection" block)

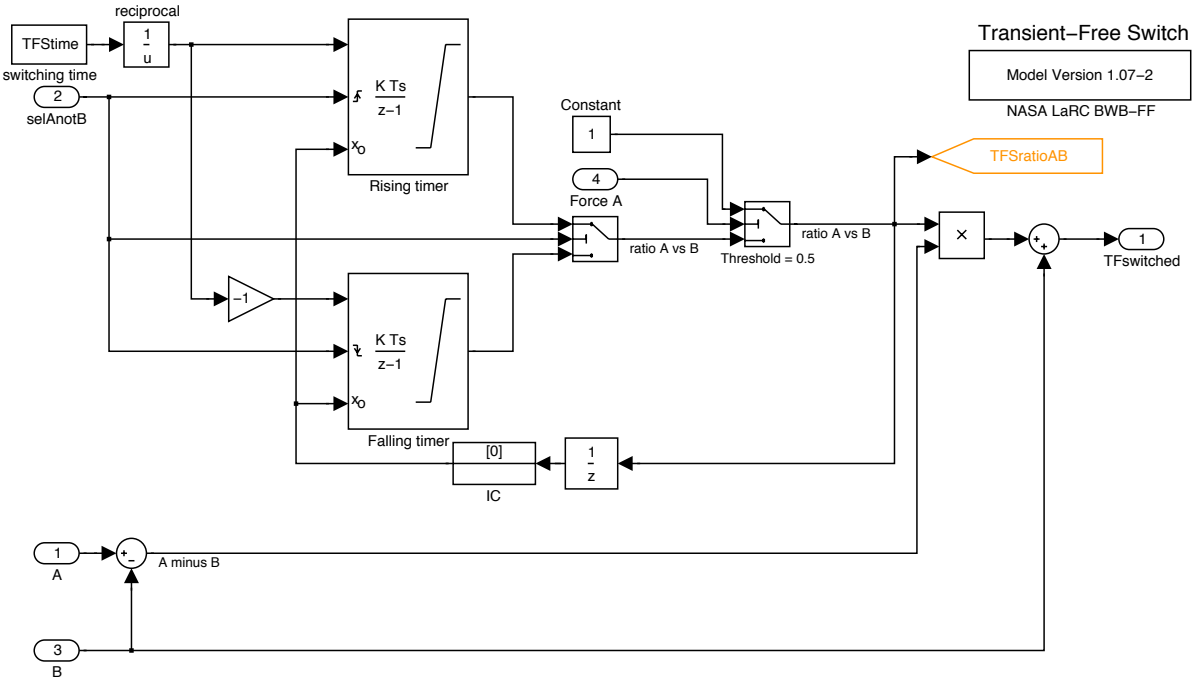

Figure 18. Transient-free switch ("Input condition + selection/Transient free switch" block)

The angle-of-attack compensation was implemented to provide artificial static stability in the pitch axis, and was structured to allow a desired value for the dimensional stability derivative M_α to be specified; this function was set to zero (i.e. `Kimd` = 0) and instead a fixed linear relationship between angle-of-attack and an elevator bias was used (elevator moved trailing-edge-down as angle-of-attack increased) as described below in section 5.4.1. This feedback path could be defeated if `Open_alpha_fb` was *true*.

The thrust compensation logic used filtered ejector pressure `avg_ejector_psi` scaled by a gain that could be scheduled on angle-of-attack, `ktde`; for these tests, `ktde` was a constant gain of −0.4. This feedback could be defeated if `Defeat_thrust_comp` was *true*. This could be accomplished by a moving a switch at the pitch pilot's control station.

A test signal, `Fixed_gains`, when *true*, caused all feedbacks to be scaled by fixed gains instead of gains scheduled on angle-of-attack.

Such test inputs as well as various intermediate signal outputs are shown by the orange or light gray blocks in these diagrams.

5.4.1 Pitch stabilization feedforward path

The structure of the control system provided a means to specify a desired pitch static stability (M_α) value. However, this 'dial-a-gain' stability capability was not used as originally planned during the tests because confidence in the preflight aerodynamics was low. Instead, by selection of values for the gain tables `Kade` and `Kimd`, a simple linear schedule of elevator deflection bias as a function of angle-of-attack was used to provide artificial pitch stability. The angle-of-attack range for the pitch stability gain tables was limited by setting the `kade_floor` parameter to −10 deg and `kade_ceil` limit to +40 deg in the "artificial Cma" block shown in figure 19.

The value of `ma_desired` was set to zero, as were the entries in the `Kimd` table; this

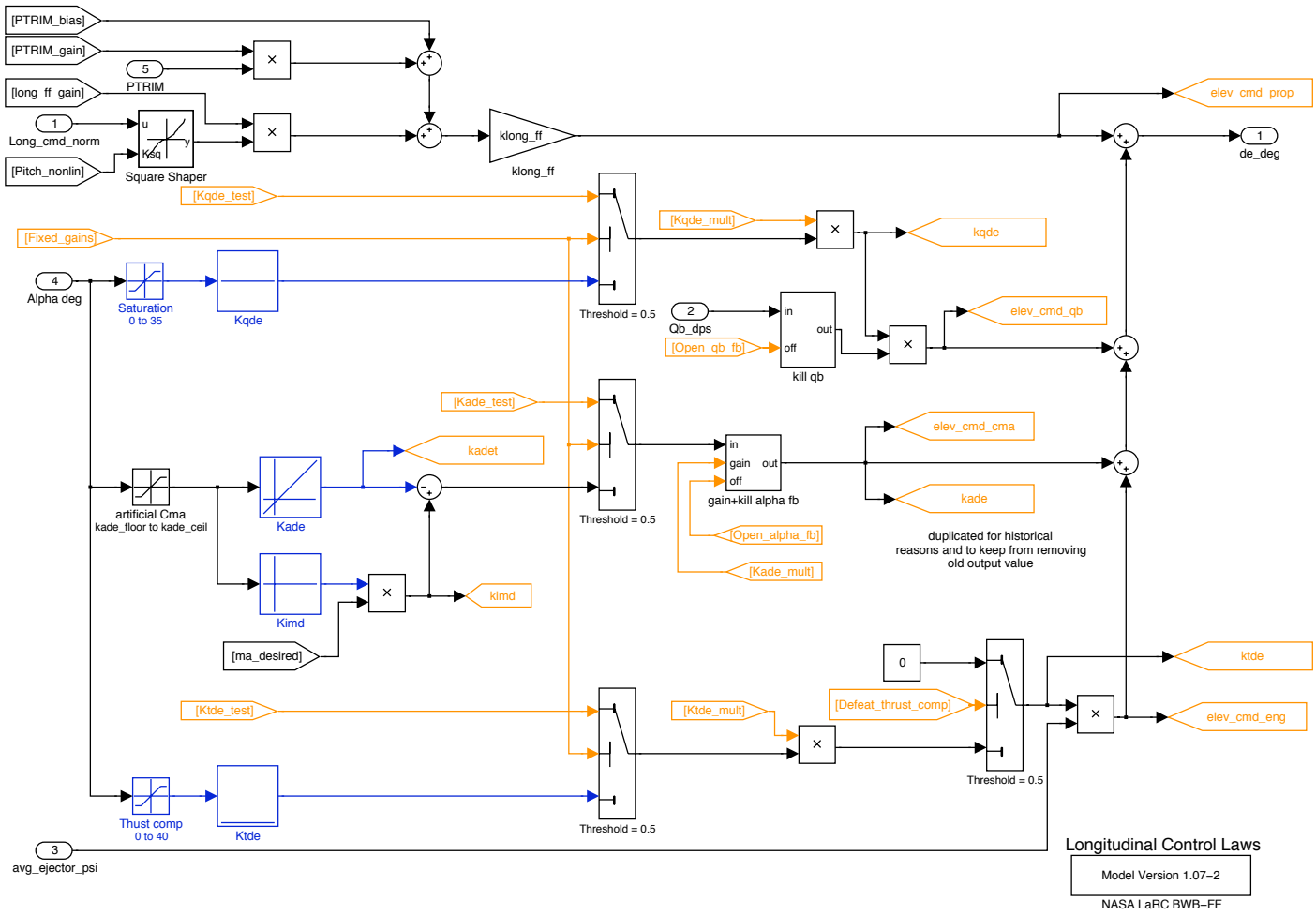

Figure 19. Longitudinal control law ("Long CLaw" block)

effectively turned off the lower additive path in the pitch stabilization feedforward logic. The values used for `Kade` given in table 12 provided a linear relationship between increasing angle-of-attack and positive (trailing-edge-down) bias of the elevator signal. (The negative sign on the summer downstream of the `Kade` block in figure 19 was offset by the negative value of `Kade_mult`).

Table 12. Longitudinal gain tables

Alpha_deg	Kqde	Kade	Kimd	Ktde
-10		-15	0	
0	0.2			-0.4
5	0.2			-0.4
15	0.2	10	0	-0.4
25	0.2			-0.4
30	0.2			-0.4
40	0.2	35	0	-0.4

5.4.2 Pitch stick input shaper

A stick signal shaper block, shown in figure 20, was provided in the longitudinal control law path to allow for non-linear shaping of the pitch pilot control input if desired, so that small stick inputs near trim would be small in magnitude but allowing for full-authority elevator command at larger inputs. By adjusting the value of input 2 (`Ksq`) the output of the block could be changed from linear ($y = u$) if `Ksq` $= 0$ to fully quadratic so that $y = u^2$ if `Ksq` $= 1$. For these tests, the local input `Ksq`, which was connected to top-level input `Pitch_nonlin`, was 0 which kept the pitch stick command linear.

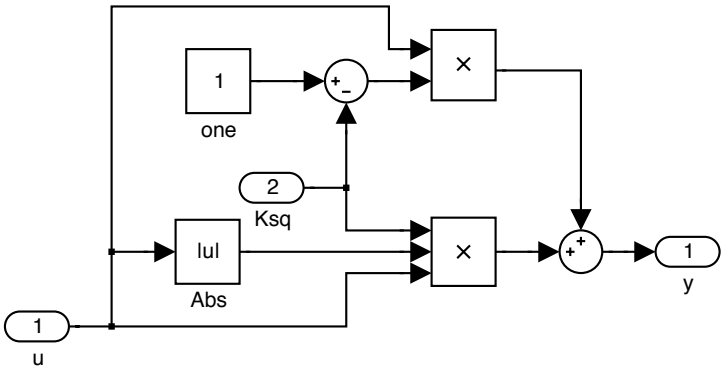

Figure 20. Pitch stick input shaper ("Long CLaw/Square Shaper") block

5.5 Lateral-Directional control law

The lateral-directional control laws, shown in figure 21, generated an aileron command based on roll rate error. The roll rate error `perr` was a function of the body roll rate input and the commanded roll rate `Pcmd_dps` that was generated from the roll pilot's lateral

command `Lat_cmd`, an adjustable feed forward gain (`lat_ff_gain`) and a fixed feed forward gain (`klatd_ff`) A rudder command was generated from filtered yaw rate and sideslip measurements and an optional aileron-to-rudder interconnection signal. Feedback gains were scheduled with angle-of-attack. Like the longitudinal law, individual feedbacks could be defeated by separate discretes, and the gain-scheduling feature could be defeated in deference to a set of fixed gains provided at run-time.

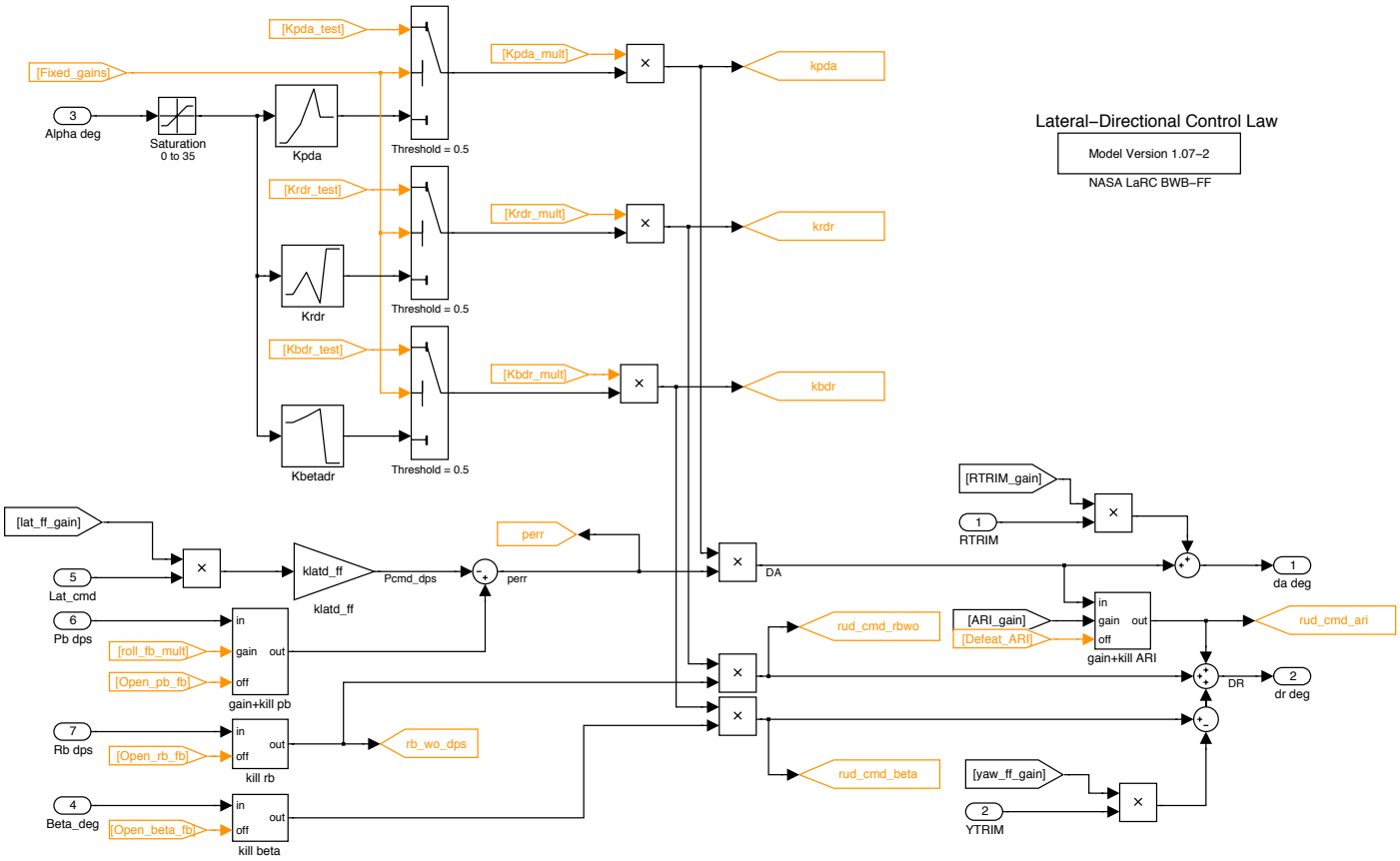

Figure 21. Lateral-Directional control law ("LatDir CLaw" block)

The filtered roll rate `Pb_dps` was multiplied by a run-time-adjustable gain `roll_fb_mult` and subtracted from the roll rate command `Pcmd_dps` to form a roll rate error signal `perr`. This error was multiplied by the roll error feedback gain `Kpda` to form signal `DA`. A run-time discrete `Open_pb_fb` could be set to defeat roll rate feedback. A roll trim signal `RTRIM`, multiplied by gain `RTRIM_gain`, was added to the `DA` signal to trim out yaw-channel biases, thus forming aileron command `da_deg`.

The rudder command `DR_deg` was generated in response to filtered body-axis yaw rate `Rb_dps`, multiplied by the yaw rate gain schedule output `Krdr` and summed with complementary-filtered sideslip feedback `Beta_deg`, multiplied by an alpha-scheduled gain `Kbetadr`. These feedbacks could be selectively turned off by run-time discretes. An optional aileron-to-rudder interconnect was provided by multiplying the unbiased aileron command by an adjustable gain `ARI_gain`; a yaw trim signal `YTRIM`, multiplied by gain `yaw_ff_gain`, was added to the rudder command to trim out biases.

Values for the lateral/directional gain functions are given in table 13 as a function of filtered angle-of-attack.

Table 13. Lateral/directional gain tables

Alpha_deg	Kpda	Krdr	Kbetadr
0	0.106	1.3	-2.71
5	0.106	1.3	-2.71
15	0.745	2.61	-1.62
25	2.0	0.792	0.0
30	1.0	3.94	-11.1
35	1.0	3.94	-11.1

5.5.1 Engine swivel algorithm

The control algorithm used to swivel the center engine is shown in figure 22. This logic provided for thrust vectoring from two potential sources: as an augmentation of the conventional rudder command (via adjustable gain `TV_dr_gain`) and directly from the roll pilot's control input `lat_cmd_norm` via adjustable gain `TV_cmd_gain`. The roll control input path was available only if the aileron-to-rudder interconnection to the rudder was not active (`Defeat_ARI` was *true*). No thrust vectoring was possible unless discrete `TV_enable_disc` was *true*, aside from a trimming signal `C_Eng_bias`. The resulting thrust vectoring command was both rate- and position-limited to form `C_eng_deg`. The rate limit was ±200 deg/s and the position limit for swiveling was ±8 deg.

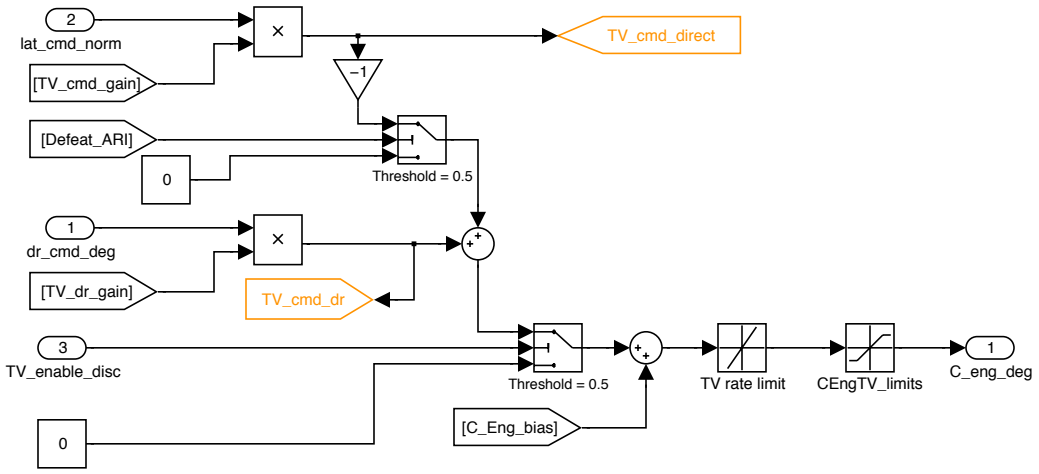

Figure 22. Engine swivel logic

5.5.2 Speedbrake logic block

Provisions were made for direct manipulation of the speedbrake control surfaces (surfaces 6-7 and 8-9 operating on each wing in a symmetric clamshell arrangement) as shown in figure 23, requiring a three-position switch to retract, hold, and extend the speedbrakes if `SB_toggle` was < 0, 0, or > 0 respectively. The extension rate was set to 2 deg/s and the retraction rate was set to 10 deg/s. The maximum extension was 60 deg; the minimum extension was set to `GAP` or 20 deg to enforce a partially-extended clamshell bias at all times.

The speedbrake command input was not exercised during these tests.

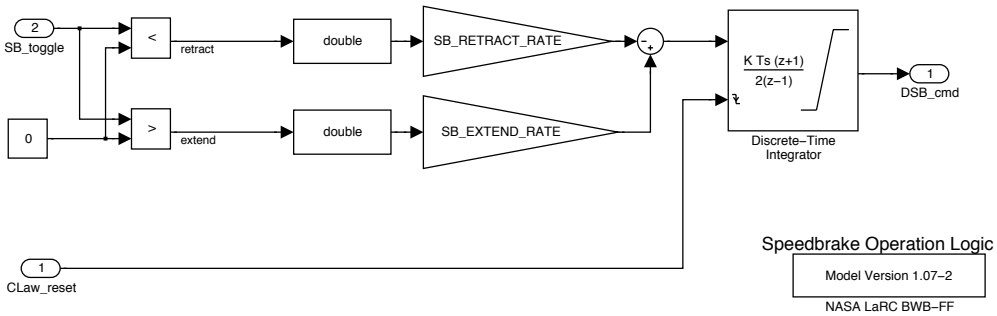

Figure 23. Speedbrake algorithm ("SB logic" block)

5.5.3 Tunnel start algorithm

A logic circuit was provided to recognize when the tunnel velocity was sufficient to use the alpha-beta sensor, as shown in figure 24. When tunnel dynamic pressure `Qbar_psf` rose above the value of `MinQ`, a boolean signal `aboveQ_unlatched` went *true*. This boolean was latched by a unit delay block to form `aboveQ`, which could be reset if input `Reset` was *true* or test input `Defeat_startup` was *true*. The latter input allowed the model's angle-of-attack and sideslip sensors to be tested with the tunnel turned off.

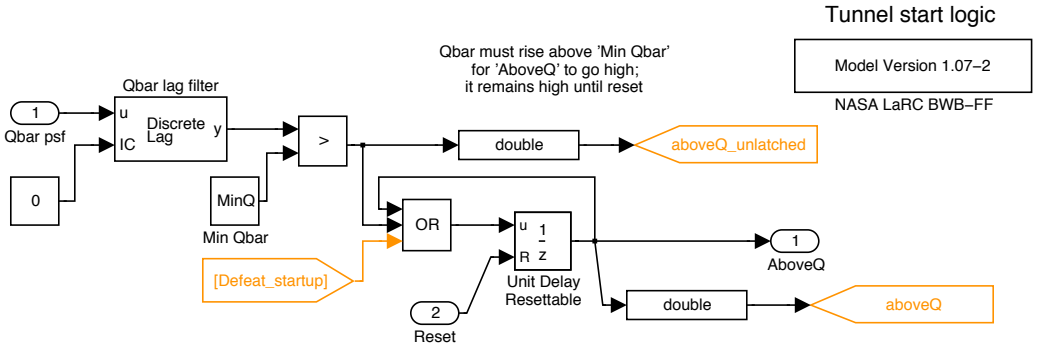

Figure 24. Tunnel start algorithm

5.6 Command output mixer logic

The mixer block (figure 25) processed the pitch, roll, yaw and speedbrake commands and distributed them to each of the various control surface actuators of the model.

Inputs to the mixer consisted of the elevator, aileron and rudder commands (`DE_cmd`, `DA_cmd`, and `DR_cmd`, respectively) and speedbrake position command (`DSB_cmd`, which was not used in these tests). The elevator and aileron commands were multiplied by surface selection vectors `DE_dist` and `DA_dist` to command the appropriate trailing edge devices

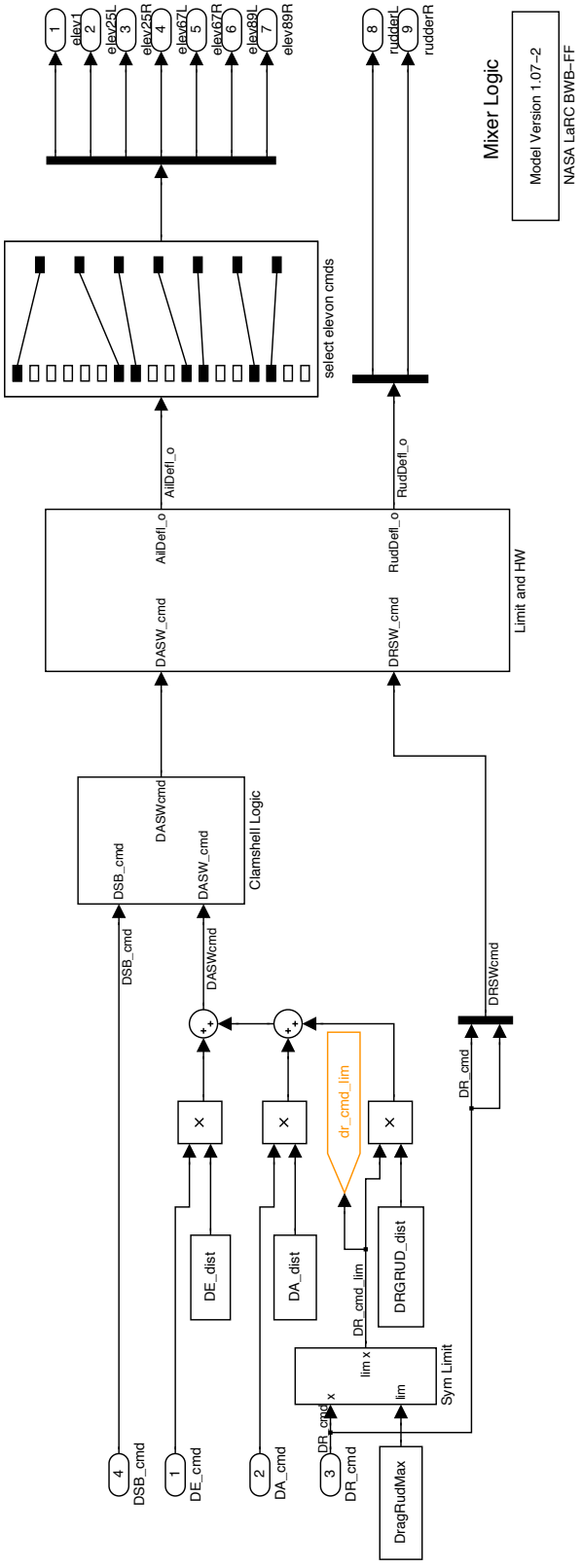

Figure 25. Command output mixer algorithm ("Mixer" block)

(assuming no surfaces were ganged; this selection was done later) in the appropriate direction; these vectors were fixed as shown:

$$\texttt{DA\_dist} = \begin{bmatrix} 0 & 0 & -1 & 1 & -1 & 1 & -1 & 1 & -1 & 1 & -1 & 1 & -1 & 1 & -1 & 1 & -1 & 1 \end{bmatrix}'$$

and

$$\texttt{DE\_dist} = \begin{bmatrix} 1 & 1 & 1 & 1 & 1 & 1 & 1 & 1 & 1 & 1 & 0 & 0 & 0 & 0 & 0 & 0 & 0 & 0 \end{bmatrix}'$$

Multiplication of these column vectors by a scalar command resulted in column vector commands where the ordering was

$$\text{command vector} = \begin{bmatrix} \text{elevon 1 left, elevon 1 right, elevon 2 left, elevon 2 right,} \ldots \\ \ldots, \text{elevon 9 left, elevon 9 right} \end{bmatrix}'$$

The values in these two distribution vectors indicate that all trailing edge devices outboard of 1 left and 1 right were deflected asymmetrically for roll and elevons 1 through 5 on each wing were deflected symmetrically for pitch.

The rudder command `DR_cmd` was limited to between ± the value of `DragRudMax` (set to 50 degrees) before being used in two paths: directly to the vertical rudders and to command the clamshell surfaces asymmetrically on either wing through the `DRGRUD_dist` distribution vector:

$$\texttt{DRGRUD\_dist} = \begin{bmatrix} 0 & 0 & 0 & 0 & 0 & 0 & 0 & 0 & 0 & 0 & 1 & -1 & 1 & -1 & -1 & 1 & -1 & 1 \end{bmatrix}'$$

This distribution used the clamshell drag rudders (surfaces 6-9) asymmetrically on either wing to provide yawing moment.

The resulting elevon command vector `DASWcmd`, the sum of the three preceding vector products, was passed into the clamshell control block, along with the speedbrake position command to form a stream-wise elevon command vector (also named `DASWcmd`). This full set of elevon commands vector and the vertical rudder command vector were then limited and converted to hinge-wise deflection commands by the Limit and HW block before selecting (from a full surface deflection command vector) the representative commands for the ganged actuators. Table 14 shows which hinge-wise elevon deflection command was chosen to drive which set of ganged control surfaces.

Table 14. Output surface command selection

Ganged surfaces set	Selected elevon command
2–5	4
6–7	6
8–9	8

5.6.1 Clamshell control

The purpose of the clamshell control block was to symmetrically superimpose the speedbrake function on top of the distributed elevon commands to clamshell surfaces 6-9 on each wing. The speedbrake command was limited to prevent saturation of any surface while guaranteeing the upper and lower control surfaces would remain at least a total of `DSB_cmd` degrees

apart. The value used for DSB_cmd in these tests was the value of GAP or 20 degrees; this large value was chosen due to data showing the upper split elevon surfaces to be ineffective at higher angles of attack and low deflection angles. Since both the upper surfaces (8-9) and lower surfaces (6-7) could be commanded beyond the 0 deflection position, this protection had to be provided to prevent damage to the actuator hardware. Figure 26 depicts this algorithm.

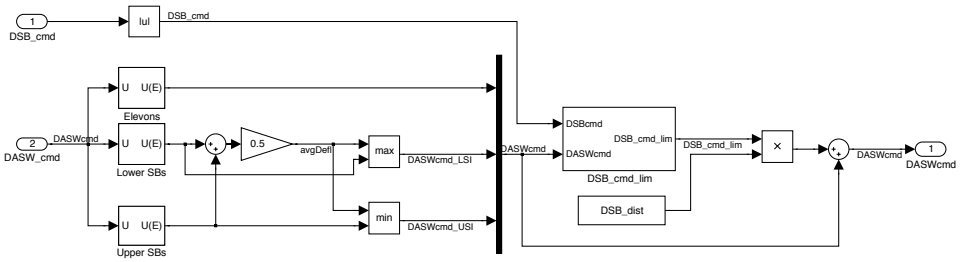

Figure 26. Clamshell control ("Clamshell logic" block)

Three selection blocks separated the stream-wise elevon command vector DASW_cmd into sub-vectors for elevon (surfaces 1-5 on each wing), lower speedbrake (surfaces 6-7 on each wing) and upper speedbrake (surfaces 8-9 on each wing) deflection commands. The upper and lower speedbrake vectors were averaged together to form a third speedbrake vector, avgDefl, which represented the mid-line or aileron deflection of the upper-lower surface pairs. This aileron deflection was then compared to the upper and lower surface deflections in a min/max block pair, ensuring the lower surfaces were commanded to a larger (more trailing-edge down) position than the upper surfaces by an amount of GAP or greater. This provided a sanity check to guard against bogus command values.

In a similar sanity check, the speedbrake position command was passed through an absolute value function to ensure it was 0 or greater.

The sanity-checked elevon command vector was reconstructed with a multiplex block and passed, along with the sanity-checked speedbrake command, into the speedbrake command limiter block DSB_cmd_lim.

The output of the speedbrake command limiter block was a scalar quantity representing the absolute value of the symmetric speedbrake command, limited if necessary to prevent saturation of any clamshell surface after the speedbrake, elevator, aileron and drag rudder commands are recombined. This scalar quantity was multiplied by the DSB_dist distribution vector:

$$\texttt{DSB\_dist} = \begin{bmatrix} 0 & 0 & 0 & 0 & 0 & 0 & 0 & 0 & 0 & 0 & 1 & 1 & 1 & 1 & -1 & -1 & -1 & -1 \end{bmatrix}'$$

to command the upper surfaces in a negative (upwards) sense and the lower surfaces in a positive (downwards) sense. This vector was then added to the sanity-checked vector representing the combined elevator, aileron and drag rudder elevon commands deflections to form the total outboard elevon commands for all trailing-edge surfaces.

5.6.2 Speedbrake command limiter

This block, shown in figure 27, calculated the maximum allowable amount of speedbrake that could be commanded, based on the combined elevator, aileron and drag-rudder command for each clamshell half (upper and lower surfaces 6-9). This block gave priority to the other three functions (elevator, aileron, drag-rudder) ahead of the speedbrake function and

ensured the speedbrake increment would be symmetrical to reduce coupling into roll, pitch and yaw motions.

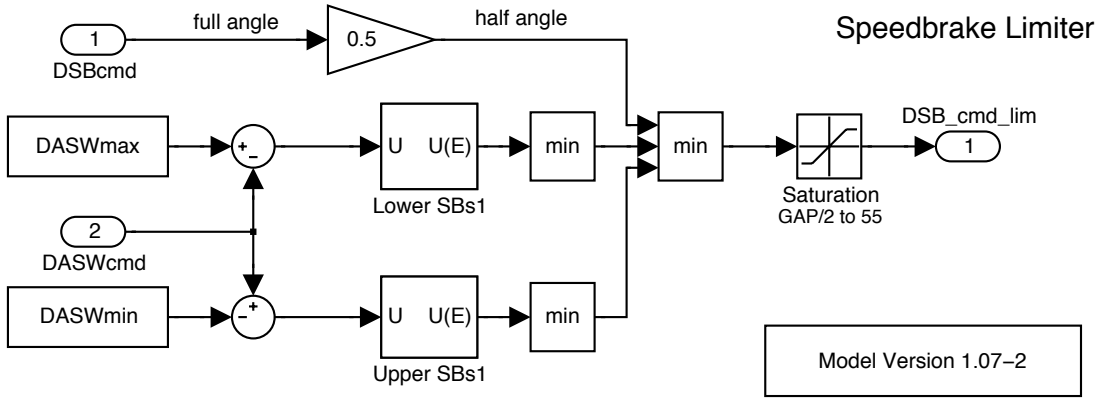

Figure 27. Speedbrake command limiter ("DSB_cmd_lim" block)

The speedbrake command limiter first calculated the available command deflection, in a stream-wise sense, for each of the upper and lower speedbrake surfaces. It then chose the minimum of this available deflection for any surface or the commanded deflection from the speedbrake command `DSBcmd`. The scalar result was then limited to ensure no more than 55 degrees and no less than half of the value of `GAP` (10 degrees was commanded). This limited minimum speedbrake value was the sole output signal from this block.

5.6.3 Speedbrake limit and conversion to hinge-wise coordinates

This block, shown in figure 28, applied limits to the stream-wise command values for each control surface (elevons and vertical rudders) before converting the stream-wise commands to hinge-wise (actuator) deflection commands. The hinge-wise command signals then passed through rate limits (200 deg/sec) and then through a final position limit for each surface.

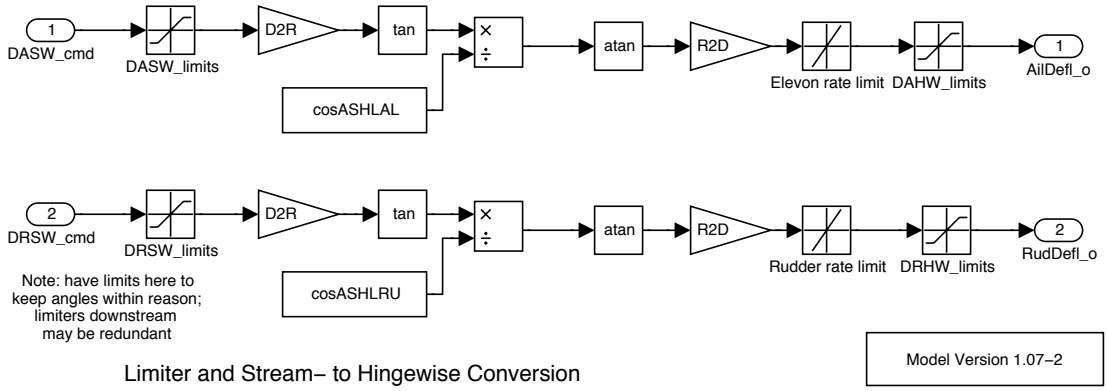

Figure 28. Speedbrake limit and conversion to hinge-wise coordinates ("Limit and HW" block)

The limits for each surface are given in table 15 in both stream-wise and hinge-wise coordinates:

Table 15. Stream-wise (SW) and hinge-wise (HW) position limits for control surfaces

Surface	SW limits	HW limits
Elevon 1	$-40 \cdots +30$	$-40 \cdots +30$
Elevon 2	$-40 \cdots +30$	$-42.4 \cdots +32.1$
Elevon 3	$-40 \cdots +30$	$-41.1 \cdots +31.0$
Elevon 4	$-40 \cdots +30$	$-40.2 \cdots +30.2$
Elevon 5	$-40 \cdots +30$	$-44.1 \cdots +33.7$
Elevon 6	$-40 \cdots +55$	$-44.1 \cdots +55$
Elevon 7	$-40 \cdots +55$	$-44.1 \cdots +55$
Elevon 8	$-55 \cdots +30$	$-55 \cdots +33.7$
Elevon 9	$-55 \cdots +30$	$-55 \cdots +33.7$
Rudder	30 (outboard) $\cdots$ 40 (inboard)	34.6 (outboard) $\cdots$ 45.1 (inboard)

5.6.4 Symmetric limiter logic

This logic, used by the mixer and shown in figure 29, was simply a symmetric limiter that limits input `x` to remain between a value of plus or minus `lim`.

6 Control law tuning

This section gives a summary of the desired set of gains and switch settings developed over the course of these tests.

During the course of the wind tunnel free-flight tests a number of gain adjustments were made to some of the control law switches and gains. These changes were based on pilot preferences and resulted in different values than the nominal values specified in table 7. The gains were manually varied as a function of tunnel dynamic pressure Q and vehicle configuration (center of gravity position, or C.G., and slats attached/detached)

Table 16 lists the configuration-specific gain settings that were set by the control system programmer based on pilot preference.

Table 16. Control law gain settings based on vehicle configuration

		Slats / C.G., % m.a.c.		
		on		off
Name	Gain Description	36	40	36
`Lat_ff_gain`	Lateral feedforward gain	1.5	2.0	0.75
`Kqde_mult`	Pitch rate to elevator feedback multiplier	2.0	4.0	2.0
`Kade_mult`	Alpha to elevator feedback multiplier	-0.5	-1.0	-1.0
`Ktde_mult`	Thrust to elevator feedback multiplier	1.5	1.0	1.5
`Kpda_mult`	Roll error-to-aileron feedback multiplier	1.0	1.0	2.0
`Krdr_mult`	Yaw-to-rudder feedback multiplier	1.0	$\begin{cases} 1.0 & \text{if } Q >= 3 \\ 0.8 & \text{otherwise} \end{cases}$	1.0

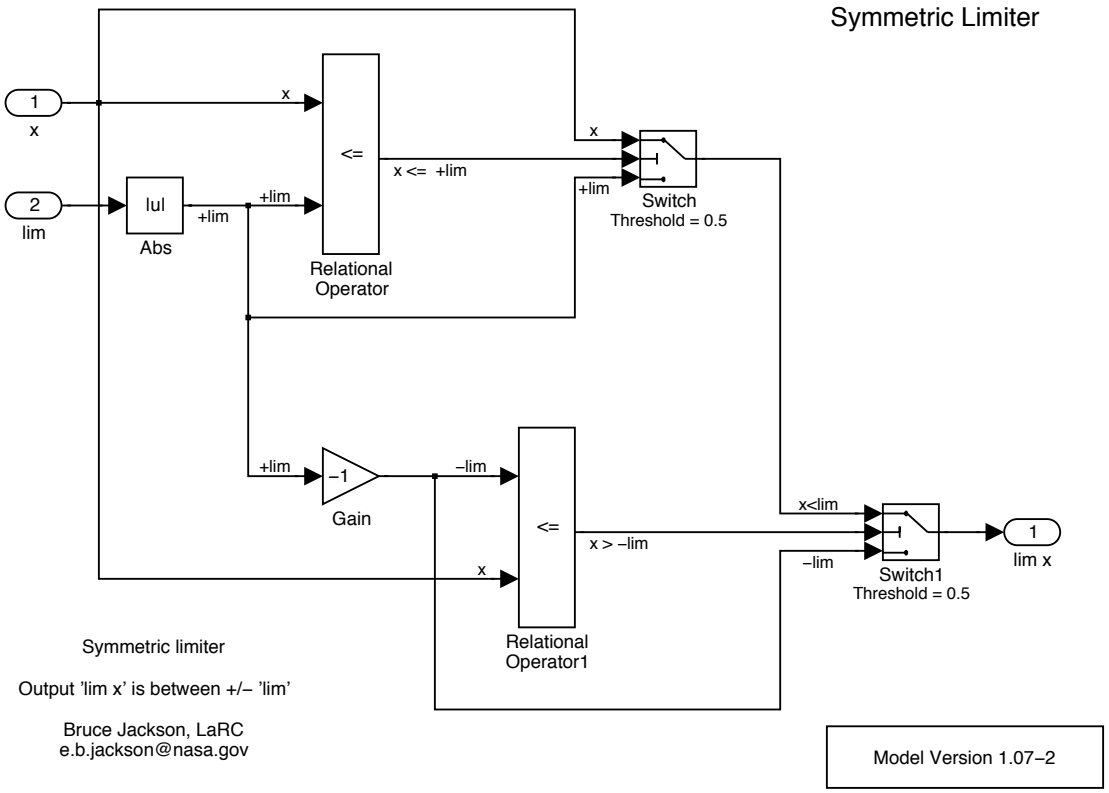

Figure 29. Symmetric limiter ("Sym Limit" block)

6.1 Gain and switch settings

6.1.1 Gain schedules

The pilots indicated that the aileron-to-rudder interconnect gain `ARI_gain` and the longitudinal feed-forward gain, or pitch stick gain `long_ff_gain` needed to be adjusted as a function of flight condition and vehicle configuration. As a result, the pilots' preferences for these two gains are shown in figures 30 and 31 as a function of tunnel dynamic pressure Q, which is measure of free-stream tunnel airspeed. In these figures, a suggested schedule that fairs through the majority of the gain preference has been manually added.

Figure 30 shows the values for `ARI_gain` that were preferred by the lateral-directional pilot for both aft and forward C.G. configurations. The forward C.G. position was tested with slats both attached and detached; no significant difference in preferred gain was noted. Also shown in the figure is a suggested gain schedule versus tunnel dynamic pressure that could be used in any future test of this control law and vehicle configuration.

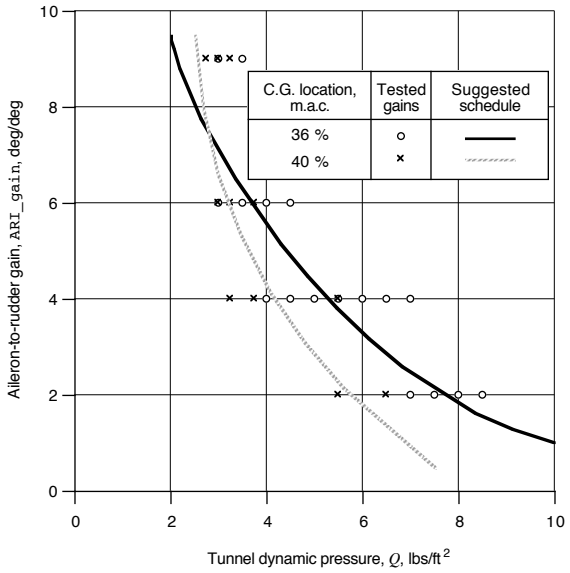

Figure 30. Test points and suggested gain schedule for aileron-to-rudder interconnection gain, `ARI_gain`, for forward and aft center of gravity locations as a function of tunnel dynamic pressure

Figure 31 shows values for the `long_ff_gain` that were preferred by the pitch pilot for both aft and forward C.G. configurations. The forward C.G. position was tested with slats both extended and retracted; no substantial difference in preferred gain was noted. Also shown in the figure is a suggested gain schedule versus tunnel dynamic pressure that could be used in any future test of this control law and vehicle configuration.

It is probable that these suggested gain schedules could be implemented as a function of either on-board airspeed sensors.

6.1.2 Switch settings

The initial tests showed that the vehicle flew better with the aileron-to-rudder interconnect (ARI) path enabled and angle-of-sideslip feedback path disabled, so `Defeat_ARI` was

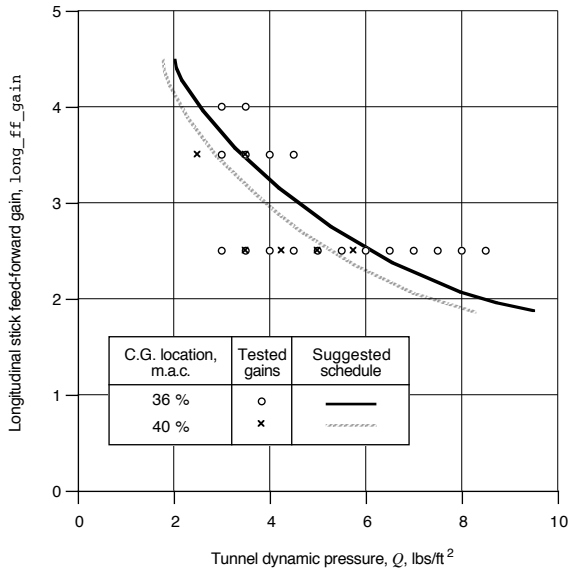

Figure 31. Test points and suggested gain schedule for longitudinal feed-forward gain, `long_ff_gain`, for forward and aft center of gravity locations as a function of tunnel dynamic pressure

normally *false* and `Open_beta_fb` was normally *true*.

The rest of the feedback signals were left enabled (meaning their corresponding `Open` and `Defeat` switches were *false*).

7 Concluding remarks

The control laws described in this report, with the gain settings and schedules described herein, could be refined with additional testing. However, the pilots have indicated that the closed-loop vehicle flown during these tests was stable and controllable in all axes.

The main control deficiencies noted were a high workload in the lateral/directional axes during slower-speed flight, and the need for considerable anticipation in the thrust axis at all times. In addition, an unexplained, seemingly random pitch perturbation was occasionally observed that kept the pitch axis workload fairly high and unpredictable; the origin of these perturbations remains unexplained.

Formal flying quality opinions, such as Cooper-Harper ratings, were not taken during these tests since a flying qualities evaluation was not the purpose of these tests.

It is likely that, based on the gain and switch settings described in the previous section, the control laws could be simplified somewhat for any future test of this vehicle. The gain schedules shown in figures 30 and 31 could be modified, by an appropriate transformation and calibration, to be functions of measured airspeed. Preferred switch settings of the lateral/directional pilot indicate that angle-of-sideslip feedback was not helpful, so this feedback could be removed. The provision to approximate a desired value of M_α was not used, so two lookup tables (`Kade` and `Kimd`) could be removed. Other lookup tables were set to constant values and thus could be replaced with simple gains. The provision to use a fixed-gain schedule was never used, so this path (with `Fixed_gains` *true*) and associated

constant gains (`Kpda_test`, etc.) could be eliminated.

The speedbrake command path was not exercised, principally due to lack of an appropriate input switch for the pitch or thrust pilot; installation of a switch would have delayed testing and testing of the speedbrake function was a low priority. As a result the associated command logic and mixer path for the speedbrake command were not tested.

The pitch and roll hold autopilot functions that were planned for this control law were not implemented so the pitch and roll sensor inputs and enable switch inputs for these two functions could be removed unless future tests require their implementation.

References

MILSTD1797. Anon: "Military Standard: Flying Qualities of Piloted Aircraft," MIL-STD-1797A, January 1990.

Jackson95. Jackson, E. Bruce: "Manual for a Workstation-based Generic Flight Simulation Program (LaRCsim) Version 1.4," NASA/TM 110164, May 1995.

REPORT DOCUMENTATION PAGE	Form Approved OMB No. 0704–0188

1. REPORT DATE *(DD-MM-YYYY)*	2. REPORT TYPE	3. DATES COVERED *(From - To)*
01-08-2006	Technical Memorandum	06/2005–11/2005

4. TITLE AND SUBTITLE

Control Laws for a Wind Tunnel Free-Flight Study of a Blended-Wing-Body Aircraft

5a. CONTRACT NUMBER

5b. GRANT NUMBER

5c. PROGRAM ELEMENT NUMBER

6. AUTHOR(S)

E. Bruce Jackson and C. W. Buttrill
Langley Research Center, Hampton, Virginia

5d. PROJECT NUMBER

5e. TASK NUMBER

5f. WORK UNIT NUMBER

7. PERFORMING ORGANIZATION NAME(S) AND ADDRESS(ES)

NASA Langley Research Center
Hampton, Virginia 23681-2199

8. PERFORMING ORGANIZATION REPORT NUMBER

L–19273

9. SPONSORING/MONITORING AGENCY NAME(S) AND ADDRESS(ES)

National Aeronautics and Space Administration
Washington, DC 20546-0001

10. SPONSOR/MONITOR'S ACRONYM(S)

NASA

11. SPONSOR/MONITOR'S REPORT NUMBER(S)

NASA/TM–2006–214501

12. DISTRIBUTION/AVAILABILITY STATEMENT

Unclassified-Unlimited
Subject Category 08
Availability: NASA CASI (301) 621-0390

13. SUPPLEMENTARY NOTES

An electronic version can be found at http://ntrs.nasa.gov.

14. ABSTRACT

This paper documents the control laws used in the free-flight tests of a 5% scaled blended-wing-body aircraft in the NASA Langley 30x60 Full-Scale Tunnel, conducted in the summer of 2005.

15. SUBJECT TERMS

BWB, blended-wing-body, free flight, free-flight, control laws, thrust vectoring

16. SECURITY CLASSIFICATION OF:			17. LIMITATION OF ABSTRACT	18. NUMBER OF PAGES	19a. NAME OF RESPONSIBLE PERSON
a. REPORT	b. ABSTRACT	c. THIS PAGE			STI Help Desk (email: help@sti.nasa.gov)
U	U	U	UU	44	19b. TELEPHONE NUMBER *(Include area code)* (301) 621-0390